minerals

MDPI

Article

Flotation-Based Separation Method for the Remediation of Marine Sediments Contaminated by Mining and Metallurgical Wastes

Giulio Sogos [1,*], Pierpaolo Manca [1], Paolo Bevilacqua [2], Alessio Lai [1], Francesco Pinna [1], Valentina Dentoni [1] and Battista Grosso [1]

[1] Department of Civil and Environmental Engineering and Architecture, University of Cagliari, Via Marengo 2, 09123 Cagliari, Italy; ppmanca@unica.it (P.M.); alessio.lai@unica.it (A.L.); francesco.pinna92@unica.it (F.P.); vdentoni@unica.it (V.D.); grosso@unica.it (B.G.)

[2] Department of Engineering and Architecture, University of Trieste, Via Alfonso Valerio 6/a, 34127 Trieste, Italy; paolo.bevilacqua@dia.units.it

* Correspondence: giulio.sogos@unica.it

Abstract

Marine sediments contaminated by mining and metallurgical activities represent a major environmental challenge, particularly in industrial port areas. This study develops and evaluates a characterisation-driven flotation flowsheet for contaminated marine sediments from the industrial harbour of Portovesme (southwestern of Sardinia, Italy). The novel contribution lies in integrating sediment mineralogical and particle-size characteristics into the arrangement of classification and sequential flotation stages, while evaluating process performance in terms of regulatory compliance, sediment recovery, and minimisation of contaminated residues rather than removal alone. Batch flotation tests were based on a conventional sphalerite flotation scheme, without a comminution stage. Three alternative process configurations were investigated by varying the position of two particle-size classification steps. The selected configuration was subsequently applied to sediments with different contamination characteristics, for a total of five treatment tests. Four of the five tests produced a decontaminated product (DP) with Zn, Pb, Cd, and Hg concentrations below the Italian regulatory thresholds for industrial sites (CTC_B). Approximately 75%–85% of the treated sediment was recovered as DP, while 15%–25% was concentrated into a non-decontaminated product (NDP). Contaminant removal efficiencies reached approximately 75% for Pb, 82% for Zn and 90% for Cd and Hg. These findings support the potential of characterisation-driven flowsheet design to recover sediments potentially suitable for beneficial reuse while concentrating contaminants into a smaller residual fraction.

Keywords: marine sediments; flotation flowsheet; selective separation; froth flotation; heavy metals; mining wastes, metallurgical wastes; particle-size classification

Academic Editors: Jianhua Chen, Xiong Tong and Ye Chen

Received: 7 October 2026
Revised: 5 November 2026
Accepted: 10 November 2026
Published: 11 November 2026

Copyright: © 2026 by the authors. Licensee MDPI, Basel, Switzerland. This article is an open access article distributed under the terms and conditions of the Creative Commons Attribution (CC BY) license.

1. Introduction

1.1. Dredging and Management of Marine Sediments

Marine sediments contaminated by mining, metallurgical and industrial activities represent one of the major environmental challenges affecting coastal and port areas

worldwide. Historically, dredging activities have been undertaken primarily to maintain navigation channels, harbour basins, and port infrastructure. Over the past few decades, however, dredging has increasingly assumed a role in environmental remediation owing to the widespread contamination of marine sediments in industrialised coastal areas [1,2]. Consequently, dredging projects are now frequently associated not only with navigational requirements but also with the management and treatment of contaminated sediments prior to their reuse or disposal [3].

Worldwide, several hundred million cubic metres of marine sediments are dredged every year. In Europe, the annual dredged volume is estimated at approximately 200 million m^3 [4–6], while in Italy about 6 million m^3 of sediments are dredged annually, of which approximately 10%–20% are contaminated [7]. The management of these contaminated materials represents a significant technical, environmental and economic challenge because the adopted strategy directly affects treatment costs, disposal requirements and opportunities for beneficial reuse.

Sediment contamination in industrial port areas is mainly associated with anthropogenic activities, including mining and metallurgical production, shipping operations and industrial or municipal wastewater discharges. The resulting pollutants comprise both organic contaminants, such as polycyclic aromatic hydrocarbons (PAHs), polychlorinated biphenyls (PCBs), pesticides and dioxins, and inorganic contaminants, particularly heavy metals including Zn, Pb, Cd and Hg [8–11]. Among these, Hg deserves particular attention because of its persistence, toxicity, bioaccumulation potential and resistance to natural degradation [12].

Traditional management options for contaminated dredged sediments include confined disposal facilities, offshore disposal and landfilling, all of which are generally associated with considerable environmental and economic costs [12].

In Italy, the management of dredged sediments is governed by different regulatory provisions depending on their origin, environmental quality and intended destination. Ministerial Decree No. 173/2016 [13] establishes criteria for the characterisation, classification and management of dredged materials, particularly in relation to marine disposal, beach nourishment and placement in confined environments, whereas specific provisions apply to sediments dredged within Sites of National Interest (SINs) under Ministerial Decree No. 172/2016 [14].

For dredged materials originating from SINs and intended for terrestrial use, the regulatory framework allows the material to be considered either as a whole or as individual particle-size fractions obtained by physical separation, including after treatments aimed at contaminant removal. Their potential terrestrial use is subject, among other requirements, to contaminant concentrations not exceeding the threshold values established by Legislative Decree No. 152/2006 [15] for the intended land use, distinguishing between residential and green areas (Category A) and commercial and industrial areas (Category B), as well as compliance with the applicable leaching-test requirements.

From a process-design perspective, this regulatory framework has an important implication: an effective remediation process should not simply maximise contaminant removal, but should recover the largest possible quantity of sediment meeting the relevant chemical quality criteria while minimising the contaminant-enriched fraction requiring controlled management or disposal. Consequently, increasing attention has been devoted to treatment technologies capable of reducing contaminant concentrations while allowing the recovery and beneficial reuse of treated sediments, in accordance with the European circular economy strategy [16].

In this context, dredged sediments can potentially be regarded as recoverable materials rather than solely as wastes, provided that the applicable environmental quality and reuse requirements are fulfilled.

Nevertheless, landfilling remains the most common management option for contaminated dredged sediments [17].

Most remediation technologies currently applied to contaminated marine sediments have been adapted from those originally developed for contaminated soils [6,18]. These include soil washing [19,20], electrokinetic remediation [21], stabilisation/solidification technologies [22], and thermal treatments for the removal of volatile contaminants such as Hg [17,23]. Their effectiveness, however, strongly depends on contaminant occurrence and sediment characteristics. In sediments affected by mining and metallurgical activities, heavy metals are frequently associated with sulphide minerals or other poorly soluble phases that exhibit limited amenability to conventional chemical extraction.

Under these conditions, physical and physicochemical separation techniques derived from mineral processing may represent technically and economically attractive alternatives [18,24,25]. These include particle-size classification, magnetic separation, gravity concentration, dense-medium separation and froth flotation, all of which exploit differences in the physical or physicochemical properties of the contaminated particles to concentrate pollutants into a reduced mass fraction [26,27].

Among these techniques, flotation has proved particularly effective for the treatment of dredged materials contaminated by both inorganic pollutants and hydrophobic organic compounds [28,29], providing the basis for the process investigated in the present study.

1.2. Flotation as Remediation Technique for Contaminated Marine Sediments

Froth flotation is the most widely used separation technology in the mining industry for the beneficiation of sulphide and oxide ores, owing to its ability to selectively separate minerals according to differences in their surface properties [30–32]. The process is based on the selective attachment of hydrophobic particles to air bubbles, allowing valuable minerals to be recovered in the froth phase while hydrophilic particles remain in the pulp. Although flotation has been extensively applied in mineral processing, its use for the remediation of contaminated marine sediments has received considerably less attention. Compared to the treatment of primary minerals, the treatment by flotation of dredged materials presents some criticalities similar to those of the treatment of mine tailings, for which flotation has already been proposed as a remediation method [33].

The effectiveness of flotation for sediment remediation depends on several factors, including sediment mineralogy, particle-size distribution, contaminant speciation, and operating conditions [34]. The principal operating variables include reagent type and dosage, slurry pH, air flow rate, impeller speed, conditioning time and flotation time, all of which influence particle hydrophobicity, bubble–particle attachment and, ultimately, process selectivity [35].

Unlike conventional mineral beneficiation, where process optimisation is primarily aimed at maximising the recovery of valuable minerals, flotation applied to contaminated sediments pursues a different objective. The treatment must simultaneously reduce contaminant concentrations below the regulatory limits, maximise the recovery of reusable sediment, and minimise the amount of highly contaminated material requiring disposal. Consequently, the most efficient process is not necessarily the one achieving the highest metal recovery, but rather the one providing the best balance between contaminant removal, sediment recovery, process selectivity and overall treatment cost [5,36].

An increase in collector dosage or the adoption of more aggressive operating conditions may improve contaminant recovery but often at the expense of process selectivity, leading to the recovery of larger quantities of gangue minerals through entrainment or non-selective flotation. Since the floated products generally constitute the fraction requiring disposal in hazardous waste landfills, excessive mass recovery may significantly increase the overall cost of remediation. Therefore, optimisation of flotation for

environmental applications requires a compromise between contaminant removal efficiency and minimisation of the contaminated concentrate, considering both the characteristics of the sediment and the intended use of the treated material [36].

Compared with primary ores, contaminated marine sediments present several characteristics that adversely affect flotation performance. One of the most important is particle-size distribution. Industrial flotation circuits generally achieve their highest efficiencies for particles in the approximate size range of 30–150 μm [37]. Marine sediments exhibit variable particle-size distributions, ranging from fine-grained deposits with median particle sizes (d50) of 4–25 μm to coarser dredged sediments containing appreciable proportions of particles finer than 63 μm, with silt-sized fractions (2–50 μm) frequently predominating in some harbour environments [38–40]. Similar to what has been observed during the flotation of mine tailings, these fine fractions reduce flotation efficiency because of their lower probability of bubble–particle collision and attachment, their greater tendency to be mechanically entrained into the froth and their higher specific surface area, which increases reagent consumption [41–45].

Besides particle size, the distribution of metals among different mineralogical and geochemical phases strongly influences flotation performance. Vanthuyne et al. [26] identified three major factors limiting the flotation of contaminated sediments: (i) the simultaneous occurrence of metals in sulphide and oxidised forms; (ii) the distribution of contaminants over a wide particle-size range; and (iii) the high organic matter content, which may adsorb onto mineral surfaces and reduce collector adsorption, thereby decreasing flotation selectivity.

For this reason, the mineralogical occurrence and geochemical speciation of contaminants should be carefully evaluated before selecting the most appropriate remediation strategy. Sequential extraction procedures provide valuable information on the association of heavy metals with the different sediment phases and, consequently, on their potential mobility and removability.

Metals occurring in dissolved or exchangeable forms are generally more amenable to chemical extraction, whereas those incorporated into discrete mineral particles can be more effectively removed by physical separation processes. Depending on contaminant speciation, these approaches may also be combined sequentially within an integrated treatment process [11,46].

Flotation is particularly suitable when heavy metals occur as sulphide minerals. These phases are generally resistant to acid leaching but exhibit natural hydrophobicity and can therefore be effectively recovered by flotation [34]. However, contaminated sediments frequently contain mixtures of sulphide, oxide and carbonate phases. In such cases, flotation performance can be improved through sulphidisation, which converts oxidised mineral surfaces into sulphide-like surfaces capable of adsorbing conventional thiol collectors [26,47,48].

Previous laboratory investigations have demonstrated the potential of flotation for sediment remediation. Cauwenberg et al. [28] reported removal efficiencies approaching 80% for Zn, Pb, Cu and Cd while concentrating contaminants into approximately 30% of the treated sediment mass. The Authors also observed that flotation selectivity was maximised at pH values between 8 and 9, whereas higher pH values increased overall recovery but reduced process selectivity. Furthermore, the use of kerosene as an auxiliary collector improved the flotation of sulphide particles coated by organic matter.

Veetil et al. [49] investigated the treatment of marine sediments contaminated with copper and polycyclic aromatic hydrocarbons (PAHs) by combining particle-size classification with flotation. Their results demonstrated that a three-stage flotation circuit could remove approximately 70% of Cu and more than 80% of PAHs from the sediment fraction

finer than 250 μm, enabling approximately 70% of the treated material to meet the criteria for beneficial reuse.

Similarly, Rahman et al. [50] applied flotation to river sediments contaminated by heavy metals and identified pH 5 as the optimum operating condition. Using diesel oil and potassium ethyl xanthate as collectors, the Authors achieved approximately 88% Zn removal while recovering a reusable sand fraction representing more than 60% of the initial sediment mass.

Although these studies clearly demonstrate the technical feasibility of flotation for sediment remediation, they mainly focus on the optimisation of flotation conditions and contaminant recovery. Comparatively little attention has been devoted to the development of integrated treatment flowsheets designed to achieve regulatory compliance while simultaneously maximising sediment recovery and minimising the quantity of contaminated residues requiring disposal. This aspect is particularly relevant in industrial port areas, where treatment performance must be evaluated not only in terms of contaminant removal but also with respect to the final destination of both the treated sediment and the residual concentrate.

1.3. Research Gap and Objectives

Previous studies have largely investigated the optimisation of individual flotation parameters, such as reagent dosage, slurry pH, flotation time and reagent schemes. The development of integrated treatment flowsheets addressing the broader objectives of sediment remediation remains less explored. In particular, an effective treatment strategy should achieve regulatory compliance while maximising the recovery of sediment suitable for beneficial reuse and minimising the contaminant-enriched fraction requiring controlled disposal.

Furthermore, the role of sediment characterisation in guiding process design has received limited consideration. Particle-size distribution, mineralogical composition, contaminant occurrence and geochemical partitioning strongly influence the applicability and effectiveness of physical separation processes, yet these characteristics are rarely used to systematically define the sequence and function of the individual unit operations within flotation-based remediation circuits. As a result, flotation is often treated as an isolated separation technique rather than as one component of an integrated remediation process.

The design of such integrated processes requires a detailed understanding of contaminant occurrence within the sediment matrix. Dissolved metal ions, such as Zn^{2+}, Pb^{2+} and Cu^{2+}, may interact with sediment constituents through adsorption onto clay minerals, Fe–Mn (oxyhydr)oxides and organic matter, or through precipitation as secondary mineral phases. Metals may also occur within discrete sulphide or oxidised mineral particles [8,51]. These associations directly influence flotation behaviour, since the removal of metal contaminants depends on the surface properties and floatability of their host particles. Metals associated with hydrophilic fine particles may exhibit limited selective recovery or be transported into the froth through mechanical entrainment, whereas sulphide-bearing particles can be selectively recovered through appropriate surface conditioning. Furthermore, dissolved metal ions may modify mineral surface chemistry and collector adsorption, as demonstrated by the activation of sphalerite by Cu^{2+} [26,52]

Particle-size distribution influences both contaminant concentration and flotation efficiency, whereas mineralogical association and geochemical partitioning determine the applicability of physical and chemical remediation techniques [26,46]. Consequently, sediment characterisation should not be considered merely a preliminary analytical step but an essential component of process design, providing the information required to define

the most appropriate sequence of unit operations and optimise the overall treatment strategy.

Against this background, the present study develops and experimentally evaluates an integrated flotation-based separation process for the remediation of marine sediments contaminated by mining and metallurgical wastes from the industrial harbour of Portovesme (southwestern Sardinia, Italy). The proposed treatment strategy adapts a conventional sphalerite flotation circuit to the physical, mineralogical and geochemical characteristics of the investigated sediments by integrating particle-size classification with sequential flotation stages targeting naturally hydrophobic materials, sulphide minerals and oxidised mineral phases.

Three alternative laboratory-scale process configurations were investigated, and their performance was evaluated in terms of contaminant removal, sediment recovery, contaminant distribution and compliance with the contamination threshold concentrations established by Italian legislation for industrial land use. Compliance with total-concentration thresholds is used in this study as an indicator of the potential for terrestrial reuse in industrial areas; however, actual regulatory suitability for such reuse would additionally require verification of leaching behaviour and the other site-specific requirements established by the applicable legislation.

Particular attention was devoted to identifying the process configuration showing the most favourable balance between contaminant removal, recovery of potentially reusable sediments and minimisation of the residual fraction requiring controlled disposal. This strategy is consistent with the broader objective of reducing disposal requirements and promoting the beneficial reuse of dredged materials within a circular-economy framework.

2. Materials and Methods

2.1. Study Area and Experimental Rationale

The study was conducted on marine sediments collected from the industrial harbour of Portovesme, located in southwestern Sardinia (Italy), within a Site of National Interest (SIN) designated for environmental remediation because of the severe contamination resulting from decades of mining and metallurgical activities.

According to the current port development programme, approximately 0.5 Mm^3 of sediments must be dredged to increase the harbour water depth from 3.5 m to 11.5 m. However, dredging operations are constrained by the presence of a contaminated surface sediment layer whose concentrations of several heavy metals exceed the CTCs established by Italian environmental legislation [15].

The remediation of these sediments represents a significant engineering challenge because the selected treatment process must simultaneously achieve environmental compliance, maximise the recovery of potentially reusable material, and minimise the quantity of contaminated residues requiring disposal. The latter aspect is particularly important because the economic sustainability of sediment remediation depends not only on contaminant removal efficiency but also on the volume and classification of the residual waste generated during treatment.

Among the contaminants identified during the site characterisation campaign, Zn is the predominant pollutant and occurs mainly as sulphide minerals, although a smaller proportion is present in oxidised forms. This mineralogical association makes flotation a potentially suitable remediation technology, while also requiring process configurations capable of recovering both sulphide and oxidised mineral phases. For this reason, the experimental programme was developed by adapting a conventional sphalerite flotation circuit to the treatment of contaminated marine sediments through the integration of particle-size classification and sequential flotation stages.

https://doi.org/10.3390/min16111175

The investigation was designed not only to assess the technical feasibility of flotation for sediment remediation but also to evaluate alternative process configurations in terms of contaminant reduction and sediment recovery, using the regulatory concentration thresholds relevant to potential reuse in industrial areas as chemical performance benchmarks.

Particular attention was devoted to the influence of particle-size classification on process performance, with the objective of identifying the treatment configuration that maximises sediment recovery while concentrating contaminants into the smallest possible residual fraction.

Table 1 reports the CTCs established for residential and green areas (CTC_A) and for commercial and industrial areas (CTC_B) for Zn, Pb, Cd and Hg.

Table 1. Contamination threshold concentrations (CTCs) established by Italian legislation for Zn, Pb, Cd and Hg according to land use (CTC_A = residential and green areas; CTC_B = commercial and industrial areas).

Land Use	Contamination Threshold Concentration CTC (mg kg^{-1})			
	Zn	Pb	Cd	Hg
A: Residential and green areas (public and private)	150	100	2	1
B: Commercial and industrial areas	1500	1000	15	5

These four elements were selected as target contaminants because their concentrations exceeded the CTC_B threshold values during the site characterisation campaign and therefore represented the principal remediation targets throughout the experimental programme.

2.2. Sampling

Marine sediments were collected from the Portovesme industrial harbour (Portoscuso, southwestern Sardinia, Italy, Figure 1) as part of the site characterisation programme conducted prior to the planned dredging operations. The sampling activities were carried out by AQA S.r.l. within the framework of a site investigation programme commissioned by the Consorzio Industriale Provinciale Carbonia-Iglesias.

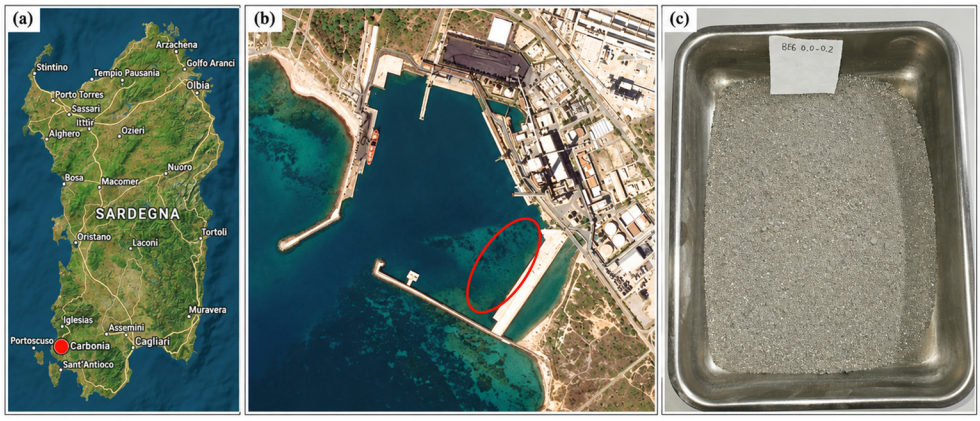


Figure 1. Study area and investigated marine sediments: (**a**) geographical location of Portovesme harbour in southwestern Sardinia (Italy), indicated by the red dot; (**b**) aerial view of Portovesme harbour, with the investigated sediment area highlighted by the red ellipse; (**c**) representative sample of the marine sediments collected from cell BE6 (0.0–0.2 m depth).

The investigated area was subdivided into three sampling cells, designated BE4, BE5 and BE6, each covering an area of 100 × 100 m. Within each cell, 16 sediment cores were

collected according to a systematic sampling layout, with regularly distributed coring locations spaced 25 m apart. Overall, 48 sediment cores, each extending to a depth of 1 m, were collected over a total area of approximately 30,000 m^2. The total amount of dry sediment collected for the experimental programme was approximately 300 kg.

Each sediment core was longitudinally divided into two equal halves. One half was retained as an archive sample for possible future investigations, whereas the other half was used for sample preparation and laboratory testing. To obtain representative materials for the experimental programme, sediments from individual cores were homogenised according to both sampling cell and depth interval, resulting in the seven composite samples listed in Table 2.

The adopted stratigraphic subdivision was designed to investigate the possible vertical variability of contaminant concentrations within the upper metre of sediment, while also allowing comparisons among the three sampling cells. Based on preliminary characterisation results indicating a different vertical distribution of contamination in cell BE4 compared with cells BE5 and BE6, cell BE4 was sampled at three depth intervals (0.0–0.2 m, 0.2–0.5 m and 0.5–1.0 m), whereas cells BE5 and BE6 were each sampled at two intervals (0.0–0.2 m and 0.2–1.0 m).

The identification codes assigned to the composite samples reflect both the sampling cell and the corresponding depth interval, as summarised in Table 2. These samples constituted the basis for the subsequent mineralogical, chemical and flotation investigations.

Table 2. Stratigraphic intervals and sample identification codes adopted for the experimental programme.

Depth	Cell		
	BE4	**BE5**	**BE6**
0.0–0.2 m	BE4_0.0–0.2	BE5_0.0–0.2	BE6_0.0–0.2
0.2–0.5 m	BE4_0.2–0.5	BE5_0.2–1.0	BE6_0.2–1.0
0.5–1.0 m	BE4_0.5–1.0		

2.3. Sediment Characterisation

2.3.1. Laboratory Procedures

Prior to the flotation experiments, the collected sediments were subjected to a comprehensive characterisation programme including particle-size, mineralogical, chemical and sequential extraction analyses. The objective of these investigations was to define the physical and chemical properties of the sediments, identify the mineralogical occurrence of the target contaminants, evaluate their distribution within the different sediment layers, and provide the information required for the design and interpretation of the flotation experiments.

Elemental analyses were performed on each of the seven composite samples described in Section 2.2 to evaluate both the spatial and stratigraphic variability of contamination within the investigated area. Major element concentrations were determined on a representative composite sample prepared by combining sediments from the three sampling cells according to their relative proportions, as described in Section 2.3.4.

Sequential extraction tests were carried out on the two surface samples (0.0–0.2 m) collected from cells BE4 and BE6, which exhibited the highest concentrations of the target contaminants during the preliminary characterisation. These analyses were performed to investigate the geochemical partitioning of the contaminants and to assess their potential removability by physical separation and chemical extraction processes.

The results of the characterisation programme provided the basis for the subsequent design of the flotation experiments, the selection of the operating conditions, and the interpretation of the treatment performance discussed in the following sections.

2.3.2. Particle Size and Mineralogical Characterisation

The particle-size distribution of the seven composite sediment samples was determined by wet sieving using sieves. The sediment was progressively separated into particle-size fractions according to the nominal aperture of the sieves, and each retained fraction was subsequently collected, dried and weighed, and the particle-size distribution was expressed as the cumulative percentage passing through each sieve aperture on a mass basis. The analysis was performed to evaluate the spatial and stratigraphic variability of sediment texture and to assess its potential influence on the subsequent flotation process. The results are presented and discussed in Section 3.1.1.

XRD analysis was performed on aliquots of the sulphide concentrate obtained by flotation of the representative composite sample BE4_BE5_BE6, which were dried and ground to <75 μm using an agate jar. Measurements were carried out using a Rigaku X-ray diffractometer with Cu–Kα radiation and a Ni filter, operated at 30 kV and 30 mA. Diffraction patterns were collected over a 2θ range of 10–60°, and the mineral phases were identified by comparison with available crystallographic reference databases. The mineralogical characterisation was performed to identify the principal sediment constituents and to determine the mineralogical occurrence of the contaminants, thereby providing the information required for the interpretation of flotation behaviour and the selection of the most appropriate treatment strategy. The results are presented and discussed in Section 3.1.2.

2.3.3. Chemical Characterisation

The chemical characterisation programme was designed to determine both the major element composition and the concentrations of the principal trace elements associated with sediment contamination.

A representative composite sample, hereafter referred to as BE4_BE5_BE6, was prepared by combining sediments from the three sampling cells in the proportions of 40 wt.% BE4, 20 wt.% BE5 and 40 wt.% BE6, reflecting their relative contribution to the investigated area. This composite sample was used for the determination of major element concentrations, whereas trace element analyses were performed on each of the seven composite samples described in Section 2.2 to evaluate the spatial and stratigraphic variability of contamination.

Moreover, to investigate the relationship between particle size and contaminant distribution, a representative sediment sample collected from the 0.0–0.2 m layer of cell BE4 was subjected to particle-size fractionation followed by chemical analysis of each size fraction.

Major element concentrations were determined following lithium metaborate fusion. Four replicate aliquots of sample were independently prepared and analysed. Approximately 0.1 g of dried sediment was mixed with 1 g of lithium metaborate in a platinum crucible and fused at 950 °C until complete melting was achieved. After cooling, the fused bead was dissolved in 5 mL HNO_3 (supplied by Carlo Erba Reagents S.r.l., Cornaredo, Italy; concentration: 65%) and 70 mL of distilled water according to the procedure described by Boar and Ingram [53]. Distilled water was produced using Adrona Crystal EX HPLC water purification system (model EX-1101-P; resistivity > MΩ·cm; conducibilty < 0.1 μS/cm).

The resulting solution was magnetically stirred until complete dissolution and subsequently diluted to 200 mL with distilled water. Major elements were determined using

a PerkinElmer Optima 7000 DV ICP-OES spectrometer (PerkinElmer, Shelton, CT, USA), and are reported as oxide weight percentages (wt.%).

Loss on ignition (LOI) was determined in accordance with EN 15935 [54] by heating approximately 1 g of dried sediment at 550 °C for 1 h and calculating the corresponding mass loss.

Trace element concentrations were determined following microwave-assisted acid digestion according to the USEPA Method 3052 [55]. Approximately 0.25 g of sample (<75 μm) was digested using a mixture of 9 mL of HNO_3 and 3 mL of HF (supplied by Carlo Erba reagents; concentration: 40%) in sealed Teflon vessels within a Milestone Start D microwave digestion system.

Concentrations of Ni, Cu, total Cr, As, Zn, Pb, Cd and V were determined by ICP-OES, whereas Hg was analysed using a PerkinElmer FIMS 100 cold vapour atomic absorption spectrometer (CV-AAS; PerkinElmer, Shelton, CT, USA). Each sediment sample and each flotation product were independently digested and analysed in quadruplicate. Procedural blanks were subjected to the same analytical procedure and were also analysed in quadruplicate to monitor potential contamination, with all target elements showing concentrations below the respective detection limits. Reported concentrations represent the mean of four independent determinations, with analytical variability expressed as standard deviation.

Major and trace element concentrations were determined as described above. The analytical results are presented and discussed in Section 3.1.3.

2.3.4. Sequential Extraction

Sequential extraction was performed to investigate the geochemical partitioning of the target contaminants and to evaluate their potential mobility and removability by different remediation techniques.

The analyses were carried out on the two surface sediment samples (0.0–0.2 m) collected from cells BE4 and BE6, which exhibited the highest concentrations of the target contaminants during the preliminary characterisation.

The extraction procedure followed the modified BCR (Community Bureau of Reference) sequential extraction protocol [56]. This method fractionates metals into operationally defined geochemical phases, thereby providing information on their binding mechanisms within the sediment matrix and on their potential response to physical and chemical treatment processes.

For each extraction, 1 g of dried sediment was used. All sequential extractions were independently performed in quadruplicate for each sediment sample, with each replicate undergoing the complete extraction procedure separately. Reagent blanks were processed together with the samples to monitor potential contamination during the extraction procedure. In Step 1, 40 mL of 0.11 mol L^{-1} acetic acid (supplied by Carlo Erba reagents; concentration: 99%) was added to the sample, and the suspension was shaken overnight, after which the extract was separated from the solid residue by centrifugation. In Step 2, the residue was treated with 40 mL of 0.5 mol L^{-1} hydroxylammonium chloride adjusted to pH 1.5 with nitric acid, and the extraction was carried out under the same conditions as Step 1. In Step 3, the residue was treated twice with 8.8 mol L^{-1} hydrogen peroxide (supplied by Honeywell Fluka; concentration: 30%) and evaporated to near dryness; 50 mL of 1.0 mol L^{-1} ammonium acetate adjusted to pH 2 with nitric acid was then added, and the extraction was performed under the same agitation and separation conditions. The residual fraction was subsequently digested with 20 mL of aqua regia.

The sequential extraction results were used to evaluate the distribution of Zn, Pb, Cd and Hg among the different geochemical fractions and to assess the suitability of alternative remediation strategies. Particular attention was devoted to distinguishing metals

potentially amenable to chemical extraction from those predominantly associated with mineral particles and therefore more suitable for removal by physical separation processes such as flotation.

2.3.5. Hierarchical Cluster Analysis

Hierarchical cluster analysis (HCA) was performed to investigate the spatial and stratigraphic variability of sediment contamination and to identify groups of samples exhibiting similar geochemical characteristics.

The analysis was based on the concentrations of the four target contaminants (Zn, Pb, Cd and Hg), selected because their concentrations exceeded the corresponding CTC_B value. To improve the statistical comparability of the variables, concentration data were standardised prior to clustering.

In addition to the seven composite samples described in Section 2.2, five supplementary samples were included in the statistical analysis to improve the representation of both spatial and stratigraphic variability. These comprised two additional surface samples from cell BE4 (designated BE4_0.0–0.2b and BE4_0.0–0.2c), one composite sample representing the weighted average of the three depth intervals in BE4 (BE4_comp), and one additional deep-layer sample (0.2–1.0 m) from cells BE5 and BE6 (designated BE5_0.2–1.0b and BE6_0.2–1.0b, respectively).

The resulting dataset comprised 12 observations (sediment samples), each described by four variables (Cd, Hg, Pb and Zn) for a total of 48 concentration values. Similarity between samples was evaluated using the squared Euclidean distance, defined by Equation (1):

$$d^2(x,y) = \sum_{i=1}^{p}(x_i - y_i)^2 \quad (1)$$

where p denotes the number of variables (p = 4), and x_i and y_i represent the standardised concentrations of the i-th analyte in the two samples being compared.

Agglomerative hierarchical clustering was subsequently applied by initially assigning each sample to an individual cluster and progressively merging the closest clusters according to the average linkage criterion. Under this approach, the distance between two clusters is calculated as the average of all pairwise squared Euclidean distances between the observations belonging to the respective clusters.

The resulting dendrogram and the corresponding cluster structure are presented and discussed in Section 3.2.

2.4. Experimental Programme

The experimental programme was designed based on the sediment characterisation results presented in the previous sections. Particular attention was devoted to the mineralogical occurrence of the target contaminants, their distribution among the different particle-size fractions, and their geochemical partitioning, as these characteristics were expected to have a direct influence on flotation performance.

The primary objective of the experimental programme was to evaluate the applicability of flotation as an integrated remediation process capable of reducing contaminant concentrations below the CTC_B values, while maximising the recovery of potential reusable sediment and minimising the quantity of contaminated material requiring disposal.

To achieve these objectives, a laboratory-scale treatment flowsheet was developed by adapting a conventional sphalerite flotation circuit to the characteristics of the investigated marine sediments. The proposed process integrates particle-size classification with sequential flotation stages targeting naturally hydrophobic materials, sulphide minerals and oxidised mineral phases. Alternative process configurations were subsequently

investigated to evaluate the influence of the particle-size classification stages on the overall treatment performance.

The experimental programme comprised laboratory-scale batch flotation tests performed under controlled operating conditions. The experimental procedure is described in Section 2.4.1, whereas the rationale underlying the different treatment configurations is presented in Section 2.4.2.

2.4.1. Experimental Procedure

Batch flotation experiments were carried out using a self-aerated Denver laboratory flotation machine equipped with a 1.5 L flotation cell, processing approximately 400 g of a representative sample per test. The initial pulp solids concentration was approximately 25 wt.%, consistent with previous flotation investigations on contaminated harbour sediments [57] and within the range of 25–32 wt.% reported for mine tailings [58–60].

Fresh tap water was used for pulp preparation. The impeller rotational speed was maintained at 1500 rpm throughout all experiments.

Three sequential flotation stages were performed to recover the different contaminant-bearing fractions. Flotation of the naturally hydrophobic fraction was carried out at the natural slurry pH (pH 7) using Dowfroth 1012 as the sole flotation reagent, acting as a frother. Sulphide flotation was subsequently performed at the same pH value, using $CuSO_4$ as an activator for sphalerite, sodium isopropyl xanthate (SIPX) as the collector, and Dowfroth 1012 as the frother. Flotation of the oxidised mineral fraction was conducted at pH 10 using Na_2SiO_3 as gangue dispersant, Na_2S as a sulphidising agent for the oxidised mineral phases, and amine MFA-15 as collector. Na_2S addition also contributed to increasing the pulp pH. Each reagent was conditioned for 1 min. The overall flotation times were 30 min for the naturally hydrophobic fraction, 25 min for the sulphide fraction, and 15 min for the oxidised mineral fraction.

These operating conditions were selected based on conventional flotation practice for zinc-bearing minerals and adapted to the characteristics of the investigated sediments.

Each flotation configuration was independently tested in duplicate (n = 2). The results are reported as mean values of the two independent flotation runs.

At the completion of each batch test, all flotation products were collected separately, dried in a ventilated oven at 30 °C for three days, and weighed to the nearest 0.01 g. The dried products were subsequently submitted to chemical analysis to determine contaminant concentrations, calculate mass distributions, and evaluate the performance of the different treatment configurations. The corresponding analytical results are presented and discussed in Section 3.3.

2.4.2. Experimental Design

The experimental programme was designed to evaluate alternative treatment flowsheets derived from a conventional sphalerite flotation circuit and adapted to the characteristics of the contaminated marine sediments investigated in this study. The design of the experimental programme was guided by the results of the sediment characterisation, particularly the mineralogical occurrence of the target contaminants, their distribution among particle-size fractions, and their geochemical partitioning, which collectively provided the basis for selecting the sequence of unit operations included in the proposed treatment process.

The adopted treatment strategy combines particle-size classification with sequential flotation stages targeting different contaminant-bearing fractions. The principal objectives were to maximise contaminant removal, maximise the recovery of sediments complying with the CTC_B values, and minimise the quantity of highly contaminated material requiring disposal.

The laboratory-scale treatment flowsheet was derived from a conventional zinc flotation circuit and consisted of the following unit operations:

- removal of the +2 mm fraction to eliminate coarse bioclastic material;
- flotation of naturally hydrophobic particles such as organic-rich particles [61];
- particle-size classification at 250 μm to separate the coarse fraction characterised by limited contamination and poor floatability;
- sulphide flotation, comprising one rougher stage followed by one scavenger stage;
- particle-size classification at 20 μm to remove the fine fraction expected to adversely affect the flotation of oxidised minerals;
- flotation of the oxidised fraction, consisting of one rougher stage followed by two scavenger stages.

Three alternative process configurations were initially investigated to assess the influence of the position of the particle-size classification stages within the treatment circuit. The configurations were tested on sediment samples selected on the basis of comparable characteristics identified during the preliminary sediment characterisation. This approach was adopted to minimise the influence of feed variability and allow a comparative assessment of flowsheet performance.

Based on this comparative assessment, the best-performing flowsheet among those investigated was subsequently applied to sediment samples characterised by different properties, in order to assess its applicability under different feed conditions.

Overall, five treatment tests were performed: three for the comparative assessment of alternative flowsheet configurations and two additional tests applying the selected flowsheet to sediments with different characteristics. The experimental tests are summarised in Table 3, while the corresponding laboratory treatment flowsheets are presented in Figure 2.

The treatment flowsheet incorporates two particle-size classification stages (250 μm and 20 μm), whose positions within the circuit were varied to evaluate their influence on process performance.

The experimental design therefore followed a two-step approach: comparative assessment of three alternative configurations under comparable feed conditions, followed by application of the selected configuration to sediments with different characteristics.

Table 3. Experimental design adopted for the five investigated treatment configurations. The grey background indicates the unit operation performed in the flowsheet.

Test ID	Cut 2 mm	Natural Hydrophobic Flotation		Cut 250 μm	Cut 20 μm	Sulphide Flotation		Cut 250 μm	Cut 20 μm	Oxide Flotation		
		Rougher	Scavenger			Rougher	Scavenger			Rougher	Scavenger	Scavenger
BE4_0.0–0.2b												
BE4_0.0–0.2c												
BE4_comp												
BE5_0.2–1.0b												
BE6_0.2–1.0b												

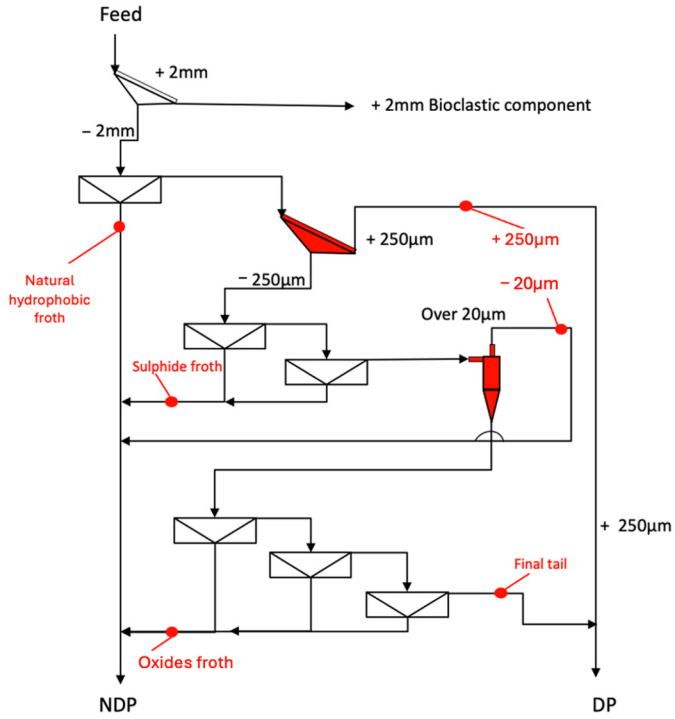


Figure 2. Laboratory-scale treatment flowsheet showing the investigated process configurations, sampling points (red dots) and product definitions. DP = decontaminated product; NDP = non-decontaminated product.

To facilitate interpretation of the treatment performance, six sampling points were established throughout the laboratory circuit (red dots in Figure 1). The collected products were subsequently combined into two final streams according to their contaminant concentrations:

- decontaminated product (DP): material complying with the CTC_B values, consisting of the final tailings together with the coarse fraction (+250 µm);
- non-decontaminated product (NDP): material exceeding the CTC_B values, comprising the concentrates recovered during the three flotation stages together with the overflow generated during the −20 µm classification step.

This classification enabled treatment performance to be evaluated directly in terms of compliance with the remediation objectives rather than solely on the basis of flotation recovery. The reagent schemes adopted for each flotation stage are reported in Table 4. Flotation reagents were prepared as aqueous solutions at the nominal concentrations reported in Table 4. Reagent dosages (g t^{-1}) were calculated relative to the dry mass of sediment treated.

For the initial comparative assessment, two aliquots (BE4_0.0–0.2b and BE4_0.0–0.2c) were obtained from the same homogenised sediment sample collected from the upper layer (0.0–0.2 m) of cell BE4 and used to investigate two alternative flowsheet configurations under equivalent feed conditions. A third sample (BE4_comp) was prepared by combining sediments from the three depth intervals of cell BE4 according to their relative proportions and was used to evaluate the third flowsheet configuration. Subsequently, sediment samples from the deeper layers (0.2–1.0 m) of cells BE5 and BE6 were selected to assess the performance of the best-performing flowsheet among those investigated under different feed conditions.

Sample identification codes reported in Table 3 indicate both the sampling cell and the corresponding depth interval. As an example, the treatment configuration applied to sample BE4_0.0–0.2b included preliminary removal of the +2 mm fraction, flotation of

naturally hydrophobic particles, particle-size classification at +250 μm and −20 μm, sulphide and oxide flotation using reagent scheme reported in Table 4.

Table 4. Reagent schemes and dosages adopted for the laboratory-scale flotation programme.

Flotation	Reagents	Manufacturer	Role	Solution Concentration	Dosage g t^{-1}	
					Rougher	Scavenger
Natural hydrophobic	Dow froth 1012	Dow Chemical Company (MI, USA)	Frother	1% (*v*/*v*)	100	50
Sulphide	Copper sulphate	Merck (Darmstadt, Germany)	Sphalerite activator	2% (*w*/*v*)	400	-
	Sodium isopropil xanthate	Dow Chemical Company (MI, USA)	Sulphide collector	1% (*w*/*v*)	100	50
	Dow Froth 1012	Dow Chemical Company (MI, USA)	Frother	1% (*v*/*v*)	100	50
Oxidised	Sodium silicate	Fisher Scientific (PA, USA)	Gangue depressant	2% (*v*/*v*)	2000	-
	Sodium sulphide	Carlo Erba Reagents (Milan, Italy)	Zn Oxide activator	5% (*w*/*v*)	4000	2000
	Amine MFA-15	Akzo Chemie (Amersfoort, The Netherlands)	Oxide collector	2% (*w*/*v*)	300	200

The effectiveness of each treatment configuration was evaluated through the chemical characterisation of the final products and by comparing mass yield (Yj) contaminant removal, metal recovery (ρi), metal removal effiencies (REi) and compliance with the CTC_B values.

The mass yield (Yj) of each flotation product was calculated as:

$$Yj = \frac{Wj}{W_F} \quad (2)$$

where Wj is the dry mass of the individual product and W_F is the mass of the feed.

The metal recovery was determined as:

$$\rho_i = \frac{C_i \cdot W_j}{CF_i \cdot W_F} \quad (3)$$

where Ci is the metal concentration of the i-th element in the j-th product and CFi is the metal concentration of the i-th element in the feed.

The contaminant removal efficiency was calculated as the fraction of the initial contaminant mass removed from the final decontaminated product (DP):

$$RE_i = 1 - \frac{CDP_i \cdot WDP}{CF_i \cdot WF} \quad (4)$$

where CDP_i and CF_i represents the concentrations of the i-th element in the DP and in the feed, respectively, while WDP and W_F represent the total mass of the DP and the feed, respectively.

For each process product, the sum of metal recoveries $\Sigma\rho i$ was calculated by adding the individual recoveries of Zn, Pb, Cd and Hg. This parameter represents the unweighted sum of the four elemental recoveries and should not be interpreted as an overall mass-weighted metal recovery.

All performance indicators are dimensionless and are reported as fractions between 0 and 1, except for $\Sigma\rho i$, which can exceed unity. The corresponding results are presented and discussed in Section 3.3.

3. Results

3.1. Sediment Characterisation

The sediment characterisation programme provided the physical, mineralogical and geochemical information required to understand contaminant occurrence and to support the design of the proposed remediation process. The results demonstrate that contaminant distribution is controlled by a combination of particle-size characteristics, mineralogical composition and geochemical partitioning, all of which directly influence the applicability and expected performance of flotation. The following sections discuss these aspects and their implications for the development of the treatment flowsheet.

3.1.1. Particle Size Distribution

The cumulative particle-size distributions of the seven composite sediment samples are presented in Figure 3 and summarised in Table 5.

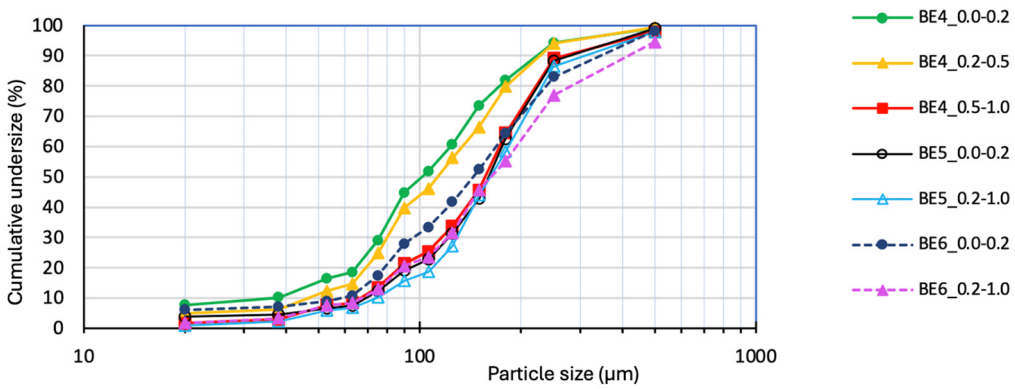


Figure 3. Cumulative particle-size distributions of the seven composite sediment samples collected from the three sampling cells.

Table 5. Characteristic particle diameters (d_{10}, d_{50} and d_{80}) of the seven composite sediment samples.

Sample	d_{10} (μm)	d_{50} (μm)	d_{80} (μm)
BE4_0.0–0.2	36	102	173
BE4_0.2–0.5	47	113	181
BE4_0.5–1.0	67	157	221
BE5_0.0–0.2	69	160	225
BE5_0.2–1.0	74	162	232
BE6_0.0–0.2	59	144	237
BE6_0.2–1.0	67	163	283

The investigated sediments exhibit noticeable spatial and stratigraphic variability in particle-size distribution. As shown in Figure 3, the proportion of fine particles progressively decreases from cell BE4 towards BE6, while a similar trend is observed with increasing sampling depth within each cell. The most pronounced differences occur between BE4 and the other two sampling cells, whereas the particle-size distributions of BE5 and BE6 are comparatively similar.

These observations indicate that the upper sediment layers, particularly within BE4, contain a larger proportion of fine material than the underlying deposits. Since fine

particles generally exhibit larger specific surface areas and a greater capacity to adsorb or incorporate heavy metals, this particle-size distribution suggests that contaminant concentrations may be influenced not only by the source of contamination but also by sediment texture.

From a process engineering perspective, the observed particle-size variability is particularly significant because particle size influences flotation performance. Fine particles are generally associated with lower flotation selectivity owing to their reduced probability of bubble–particle collision, increased entrainment into the froth phase and higher reagent consumption, as discussed in Section 1.2. Consequently, the marked differences observed among the investigated sediments justified the inclusion of particle-size classification as one of the principal unit operations of the proposed treatment process.

The particle-size distributions presented in Figure 3 therefore provided the first indication that sediment texture should be considered not only as a descriptive characteristic of the investigated material but also as a key design parameter for the development of the integrated remediation flowsheet.

3.1.2. Mineralogical Composition

Previous mineralogical characterisation of sediments from the investigated area indicated that the sediment matrix is predominantly composed of common detrital and biogenic minerals, including aragonite, calcite, quartz, albite, orthoclase, phyllosilicates and gibbsite, together with minor Fe- and Zn-bearing phases [61,62]. In the present study, XRD analysis was specifically performed on the sulphide flotation concentrate to improve the detectability of the minor contaminant-bearing sulphide phases.

The sediments were classified as bioclastic silty sands, consisting of unconsolidated, moderately sorted, medium- to fine-grained materials. The inorganic fraction is predominantly composed of aragonite, calcite, quartz, albite, orthoclase, phyllosilicates and gibbsite. In addition, iron- and zinc-bearing sulphides, mainly pyrite and sphalerite, together with iron oxides and hydroxides, were identified.

Because the concentrations of the target contaminants in the bulk sediments were relatively low for reliable identification of the corresponding mineral phases by XRD, the sulphide concentrate obtained after flotation of the representative composite sample BE4_BE5_BE6 was analysed to enhance the detectability of contaminant-bearing minerals.

The diffraction pattern presented in Figure 4 confirms the occurrence of sulphide minerals associated with Fe, Zn and Hg in the flotation concentrate. Although XRD does not provide quantitative information on the distribution of individual elements among mineral phases, the enrichment of these sulphide phases in the flotation concentrate is consistent with their recovery during sulphide flotation and supports the suitability of flotation for targeting sulphide-associated contaminants.

The mineralogical evidence therefore provides the first direct indication that the investigated contaminants are not randomly distributed within the sediment matrix but are preferentially associated with mineral phases exhibiting favourable flotation properties. This observation is consistent with the treatment strategy adopted in the present study and provides a mineralogical basis for the subsequent interpretation of flotation performance.

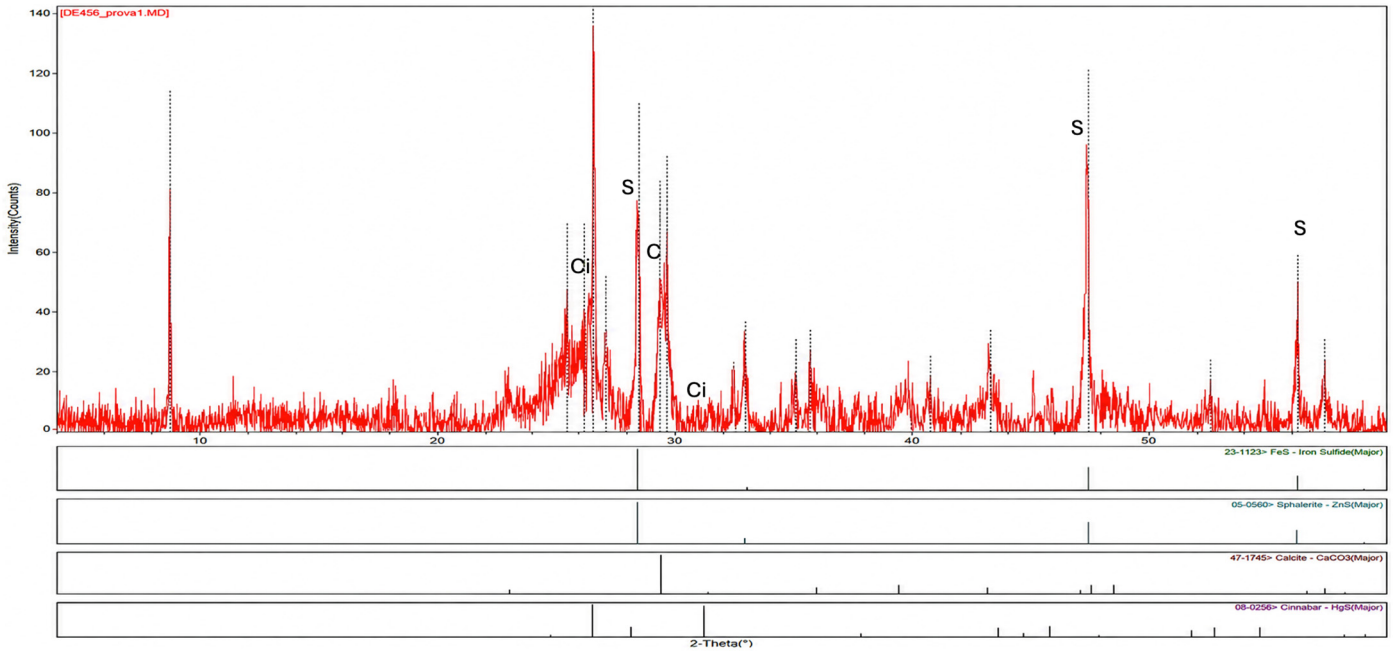


Figure 4. X-ray diffraction pattern of the sulphide concentrate obtained from the representative composite sample BE4_BE5_BE6. S = Sphalerite, C = calcite, Ci = Cinnabar.

3.1.3. Chemical Composition

The results of the chemical characterisation confirm that contamination is dominated by Zn, Pb, Cd and Hg, whereas the remaining analysed elements occur at concentrations well below the corresponding CTC_B values.

The major oxide composition of the representative composite sample is reported in Table 6, while trace element concentrations determined for the seven composite sediment samples are presented in Table 7.

Table 6. Major oxide composition of the representative composite sample BE4_BE5_BE6 (wt.%). * LOI = Loss of Ignition.

Oxide	wt.%
Al_2O_3	17.2
Fe_2O_3	3.3
MnO	0.0
MgO	1.9
CaO	11.2
K2O	2.0
Na2O	1.1
TiO_2	0.3
P_2O_5	0.1
SiO_2	48.6
LOI *	13.0
TOTAL	98.7

Table 7. Metal concentrations in the composite sediment samples from the different sampling cells and depth intervals (mg kg^{-1}). Values are pressed as mean ± standard deviation (n = 4). The red background color indicates an exceedance of the corresponding CTC_B value.

Sample	Ni	Cu	Total Cr	As	Zn	Pb	Cd	V	Hg
BE4_0.0–0.2	33.4 ± 1.2	50.7 ± 2.2	86.2 ± 3.6	<D.L.	3326.2 ± 98.4	799.3 ± 32.7	21.3 ± 0.8	70.0 ± 2.2	19.7 ± 0.5
BE4_0.2–0.5	50.1 ± 1.9	62.8 ± 0.2	87.8 ± 1.2	<D.L.	3288.5 ± 82.9	850.1 ± 21.9	24.1 ± 0.5	78.4 ± 0.8	18.2 ± 0.1
BE4_0.5–1.0	30.7 ± 0.9	43.2 ± 2.5	143.1 ± 0.6	<D.L.	3163.8 ± 53.4	1364.2 ± 28.5	26 ± 0.5	59.9 ± 1.4	20.1 ± 0.3
BE5_0.0–0.2	18.4 ± 0.2	23.1 ± 0.6	105.9 ± 4.4	<D.L.	1441.4 ± 40.1	396.8 ± 7.4	10.9 ± 0.4	39.3 ± 1.4	9.7 ± 0.2
BE5_0.2–1.0	22.9 ± 0.9	25.4 ± 1.1	103.5 ± 0.3	<D.L.	1875.8 ± 54.3	690.9 ± 3.4	15.0 ± 0.2	39.7 ± 0.9	13.5 ± 0.3
BE6_0.0–0.2	42.2 ± 1.3	53.7 ± 1.3	123.7 ± 2.4	<D.L.	3461.6 ± 44.2	833.7 ± 15.8	26.4 ± 0.7	68.1 ± 1.3	21.8 ± 0.1
BE6_0.2–1.0	36.5 ± 3.5	53.6 ± 3.6	122.1 ± 7.3	<D.L.	4407.7 ± 34.1	1687.8 ± 11.3	37.2 ± 1.9	67.0 ± 4.0	25.9 ± 0.7
CTC_A	120	120	150	20	150	100	2	90	1
CTC_B	500	600	800	50	1500	1000	15	250	5

The major oxide composition reflects the mineralogical assemblage identified by XRD, with silica and calcium oxide representing the dominant constituents of the sediment matrix, consistent with the abundance of quartz and carbonate minerals. The trace element data demonstrate that Zn, Pb, Cd and Hg are the only elements exceeding the corresponding CTC_B values in at least one of the investigated samples. However, exceedances are not systematic across the entire dataset, as some samples show Pb and Cd concentrations below the respective CTC_B values and Zn in BE5_0.0–0.2 also remains below its corresponding threshold.

These four elements represent the principal contaminants controlling the remediation strategy. The concentrations of Ni, Cu, total Cr, As and V remain below the regulatory limits in all investigated samples and therefore do not constitute limiting factors for sediment reuse.

To facilitate comparison among contaminants characterised by different regulatory threshold concentrations, the analytical results were normalised to the corresponding CTC_B values.

The length-weighted average concentrations for the three sampling cells are presented in Figure 5, whereas Figure 6 illustrates the normalised concentrations of the four target contaminants for each composite sediment sample.

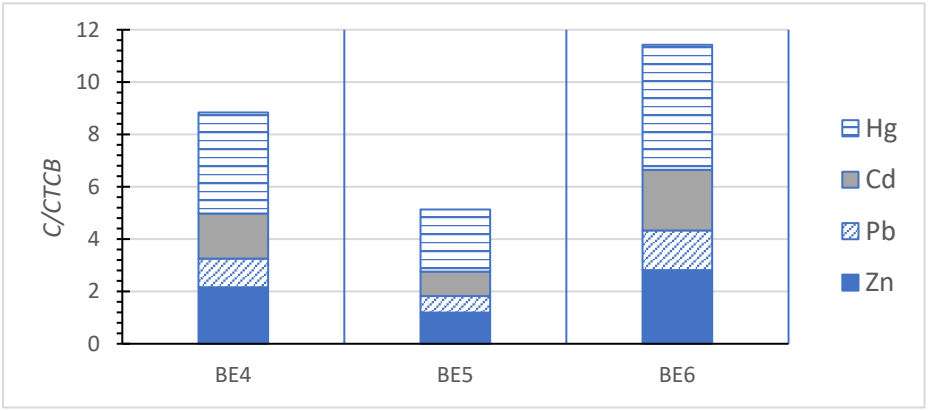


Figure 5. Length-weighted average contaminant concentrations normalised to the corresponding CTCB values for the three sampling cells.

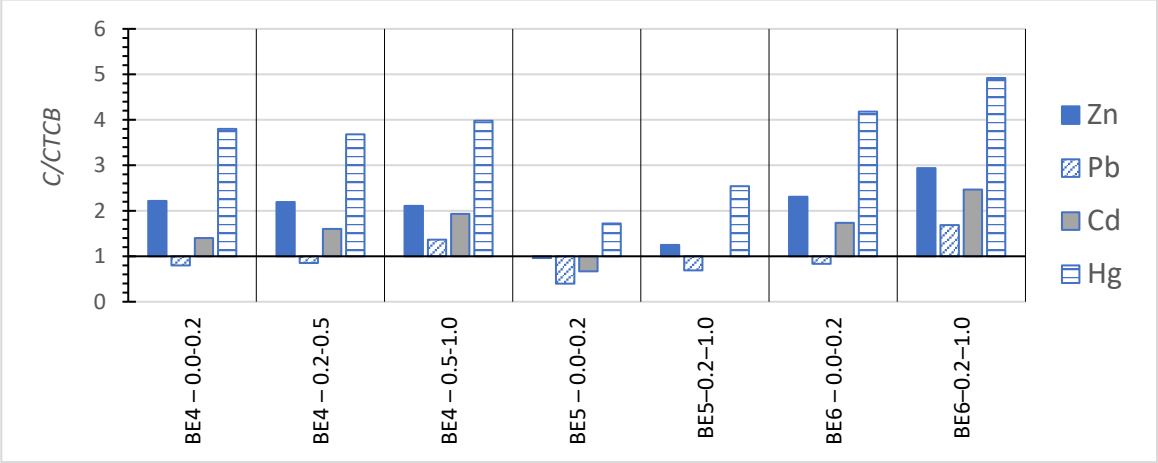


Figure 6. Normalised contaminant concentrations (C/CTCB) for the seven composite sediment samples. The horizontal axis is drawn at C/CTCB = 1 to highlight exceedances of the regulatory threshold.

Among the investigated contaminants, Hg consistently exhibits the highest normalised concentration, exceeding the corresponding CTC_B value in all sampling cells and depth intervals, and reaching values up to approximately five times the regulatory threshold in the deeper sediments of cell BE6. Zn also exceeds the regulatory threshold throughout the investigated area, with concentrations generally exceeding twice the regulatory threshold in cells BE4 and BE6 and reaching approximately three times the threshold in the deeper sediments of BE6, whereas exceedances of Pb and Cd are more variable and depend on both sampling location and sediment depth.

The comparison among sampling cells highlights a relatively homogeneous contamination pattern within BE4, whereas BE5 represents the least contaminated portion of the investigated area. In contrast, the deeper sediments of BE6 exhibit the highest concentrations of all four target contaminants, while the corresponding surface layer is characterised by contamination levels comparable with those observed in BE4.

The observed differences suggest that sediment variability cannot be adequately described solely on the basis of sampling depth. These observations provided the rationale for the hierarchical cluster analysis presented in the following section, which was performed to identify three main clustering groups of samples for the subsequent evaluation of flotation performance.

3.1.4. Distribution of Contaminant Among Particle Size Fractions

As anticipated in Section 2.3.3, to investigate the relationship between particle size and contaminant distribution, a representative sediment sample collected from the 0.0–0.2 m layer of cell BE4 was subjected to particle-size fractionation followed by chemical analysis of each size fraction.

The sample was separated into the particle-size fractions reported in Table 8, and the mass yield together with the concentrations of the target contaminants (Zn, Pb, Cd and Hg) were determined for each fraction. This characterisation was undertaken to evaluate the association of contaminants with specific particle-size classes and to provide experimental information for the design of the flotation process, particularly with regard to the selection of appropriate particle-size classification steps. The distribution of Zn and Hg among the different particle-size fractions is illustrated in Figure 7.

Table 8. Mass distribution and concentrations of Zn, Pb, Cd and Hg in the particle-size fractions of sample BE4_0.0–0.2.

Size Fraction (μm)	Yield (%)	Concentration (mg kg^{-1})			
		Zn	Pb	Cd	Hg
+250	5.74	734.1 ± 12.9	519.1 ± 2.8	6.2 ± 0.1	2.3 ± 0.1
−250 +180	12.36	2273.2 ± 35.5	819.4 ± 5.5	14.7 ± 0.6	7.6 ± 0.1
−180 +125	21.23	2194.0 ± 21.7	663.6 ± 4.1	11.4 ± 0.5	8.4 ± 0.3
−125 +75	31.70	2840.3 ± 46.2	751.9 ± 5.2	20.7 ± 1.0	17.9 ± 0.6
−75 +20	21.32	6309.1 ± 73.4	1012.4 ± 46.8	56.0 ± 1.4	27.9 ± 0.5
−20	7.66	9351.1 ± 57.0	2168.0 ± 52.3	80.3 ± 1.0	54.0 ± 2.6
Feed	100.00	3750	892	29.0	18.6
CTC_A		150	100	2	1
CTC_B		1500	1000	15	5

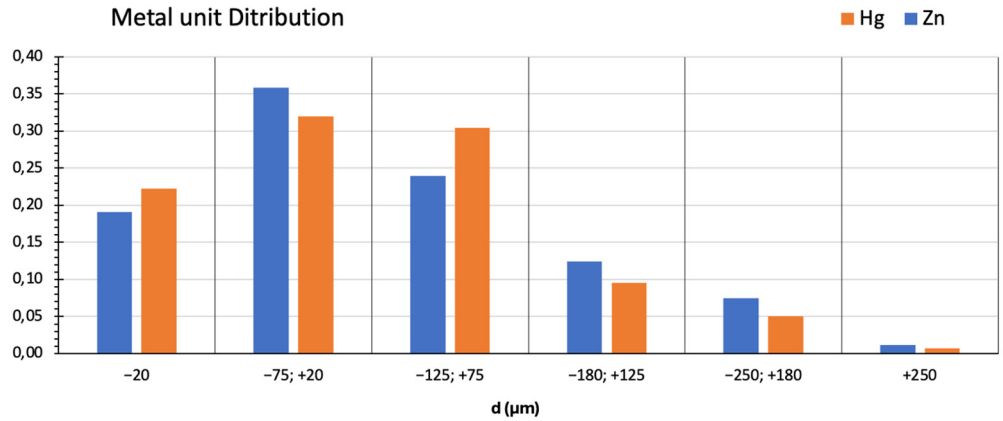


Figure 7. Distribution of Zn and Hg among the particle-size fractions of sample BE4_0.0–0.2.

The results reported in Table 8 demonstrate a clear dependence of contaminant concentrations on particle size. For all four target contaminants, concentrations increase progressively with decreasing particle size, reaching their highest values in the finest fractions. This trend is particularly evident for Zn and Hg, whose distributions closely follow each other throughout the investigated particle-size range.

Although the finest fraction (<20 μm) exhibits the highest contaminant concentrations, it represents only a limited proportion of the total sediment mass. Conversely, the −125 +20 μm fraction contains the largest proportion of both Zn and Hg owing to the combination of relatively high contaminant concentrations and its substantial mass contribution. This observation indicates that contaminant removal cannot be optimised solely by targeting the finest particles but requires consideration of both contaminant concentration and mass distribution.

The coarse fraction (+250 μm) exhibits contaminant concentrations below the corresponding CTC_B values for all four target elements. Consequently, its preliminary separation by particle-size classification makes it possible to recover a relatively clean sediment fraction without additional treatment, while simultaneously reducing the mass requiring flotation. At the opposite end of the particle-size spectrum, the very fine fraction (<20 μm) combines high contaminant concentrations with poor flotation characteristics, owing to the well-known detrimental effects of slimes on flotation selectivity discussed in Section 1.2.

These results provide direct experimental support for the inclusion of two particle-size classification stages within the proposed treatment flowsheet. The first classification stage allows the removal of the coarse fraction prior to flotation, whereas the second

eliminates the finest particles before the flotation of oxidised minerals, thereby improving both process selectivity and overall treatment efficiency [63,64].

Overall, the particle-size fractionation results demonstrate that contaminant distribution is governed by the combined effects of particle size and mass distribution, confirming that particle-size classification should be regarded as an integral component of the remediation process rather than merely as a preliminary preparation step.

3.1.5. Sequential Extraction

The sequential extraction results provide valuable information on the geochemical partitioning of the target contaminants and on their potential response to alternative remediation techniques. The distributions of Zn, Pb, Cd and Hg among the operationally defined geochemical fractions determined using the modified BCR procedure are presented in Figure 8.

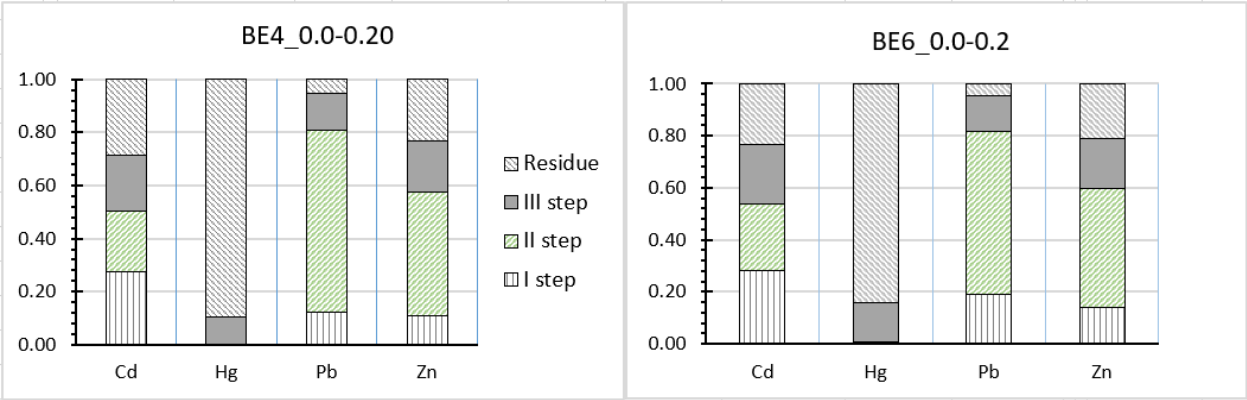


Figure 8. Geochemical partitioning of Zn, Pb, Cd and Hg in the surface sediment samples collected from cells BE4 and BE6, determined by the modified BCR sequential extraction procedure.

The two investigated samples exhibit comparable partitioning patterns despite the differences in contaminant concentrations observed between the two sampling cells. Among the analysed elements, Pb and Zn show the highest proportions associated with the more readily extractable geochemical fractions, whereas Cd displays an intermediate behaviour. In contrast, Hg is predominantly associated with the residual fraction, indicating a markedly lower mobility under the extraction conditions adopted.

The limited extractability of Hg is particularly significant from a remediation perspective. Under the conditions investigated, only approximately 10% of the mercury present in sample BE4 and 18% of that in BE6 were released during sequential extraction, suggesting limited Hg mobilisation under the investigated extraction conditions and indicating that remediation approaches relying primarily on chemical extraction may be less favourable for Hg than physical separation.

Conversely, the higher extractability of Pb and Zn suggests that these elements occur, at least in part, in more reactive geochemical forms. Nevertheless, the mineralogical analyses demonstrated that a significant proportion of the target contaminants is also associated with sulphide minerals. Taken together, these observations indicate that no single remediation technology is likely to be equally effective for all contaminants and that process selection should account for both mineralogical occurrence and geochemical partitioning.

From a process engineering perspective, the sequential extraction results reinforce the rationale for adopting flotation as the principal remediation technology. In particular, the poor extractability of Hg supports the choice of a physical separation process capable of recovering contaminant-bearing mineral particles rather than relying exclusively on

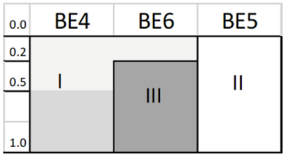
chemical extraction. Consequently, the combined interpretation of the mineralogical, chemical and sequential extraction results provides a consistent justification for the integrated treatment strategy developed in the present study.

3.2. Hierarchical Cluster Analysis

Hierarchical cluster analysis was performed to identify statistically homogeneous groups of samples based on the concentrations of the four target contaminants (Zn, Pb, Cd and Hg) and to evaluate the spatial and stratigraphic variability of sediment contamination within the investigated area.

The resulting data matrix together with the corresponding dendrogram obtained using the average linkage criterion are presented in Figure 9, while the centroid compositions of the identified clusters, expressed as contaminant concentrations normalised to the corresponding CTC_B values, are shown in Figure 10.

N.	ID	Zn	Pb	Cd	Hg
1	BE4_0.0-0.2a	3326	799	21.3	19.0
2	BE4_0.0-0.2b	4176	883	28.7	11.6
3	BE4_0.0-0.2c	3488	930	23.8	12.4
4	BE4_0.2-0.5	3288	850	23.8	18.4
5	BE4_0.5-1.0	3163	1364	28.8	19.9
6	BE4_comp	3361	1206	28.7	14.8
7	BE5_0.0-0.2	1441	396	10.0	8.6
8	BE5_0.2-1.0a	1875	690	14.8	12.7
9	BE5_0.2-1.0b	1903	688	15.0	12.7
10	BE6_0.0-0.2	3461	833	26.2	20.9
11	BE6_0.2-1.0a	4407	1687	37.0	24.6
12	BE6_0.2-1.0b	4393	1712	40.6	17.5



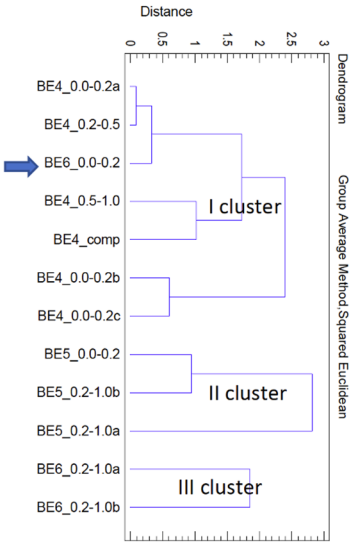


Figure 9. Hierarchical clustering of the investigated sediment samples based on the concentrations of Zn, Pb, Cd and Hg (expressed in mg kg^{-1}). The figure includes the corresponding data matrix and dendrogram obtained using the average linkage criterion.

The dendrogram reveals a relatively limited range of squared Euclidean distances ($d^2 < 3$), indicating an overall geochemical similarity among the investigated sediments despite the observed differences in contaminant concentrations. Nevertheless, the analysis identifies three statistically distinct clusters that reflect both spatial and stratigraphic variations within the study area.

Cluster I includes all samples collected from cell BE4, irrespective of depth, together with the surface sample from BE6 (0.0–0.2 m). This grouping indicates that the contamination pattern within BE4 is remarkably homogeneous throughout the investigated sediment column and that the upper layer of BE6 exhibits geochemical characteristics comparable with those of BE4.

Cluster II comprises all samples collected from BE5, again showing no significant stratigraphic differentiation within the clustering structure. This result confirms that BE5 represents the least contaminated portion of the investigated area and that contaminant variability within this sampling cell is limited.

In contrast, Cluster III consists exclusively of the deeper samples (0.2–1.0 m) from cell BE6, clearly identifying this sediment interval as the most contaminated portion of the

investigated site. The separation of these samples from the remaining dataset reflects consistently higher concentrations of all four target contaminants.

The cluster centroids presented in Figure 10 further illustrates these differences. Whereas Cluster II is characterised by the lowest normalised concentrations of all contaminants, Cluster III exhibits the highest values, particularly for Zn, Cd and Hg. Cluster I represents an intermediate level of contamination, confirming the substantial geochemical similarity among the samples grouped within this cluster.

An important outcome of the cluster analysis is that stratigraphic variability is not uniform throughout the investigated area. In cells BE4 and BE5, contamination does not vary significantly with depth, suggesting that sediment characterisation and treatment can reasonably be based on representative composite samples. Conversely, cell BE6 exhibits a marked vertical differentiation, with the deeper sediments forming a separate cluster characterised by higher contamination levels.

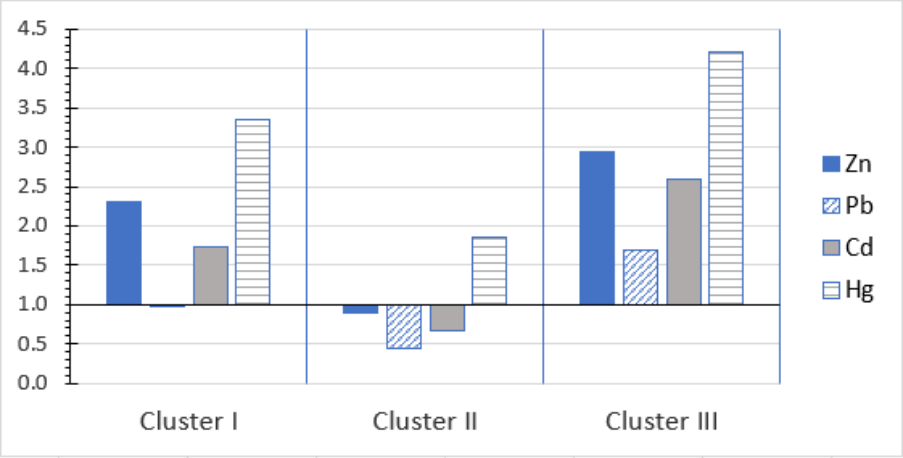


Figure 10. Cluster centroids expressed as contaminant concentrations normalised to the corresponding CTCB values. The horizontal axis is drawn at C/CTC_B = 1 to highlight exceedances of the regulatory threshold.

These results provide useful guidance for both sediment characterisation and process evaluation. The identification of homogeneous groups confirms that the variability in sediment contamination cannot be interpreted solely on the basis of sampling depth but also reflects significant lateral heterogeneity across the study area. Consequently, the HCA was used as an exploratory tool to support the selection of representative feed samples for the flotation tests.

3.3. Performance of Integrated Flotation Process

The laboratory-scale experimental programme was designed to evaluate the effectiveness of the proposed integrated remediation process under different treatment configurations derived from a conventional sphalerite flotation circuit. Process performance was assessed not only in terms of contaminant removal but also with respect to sediment recovery, mass distribution, metal recovery and compliance with the contamination threshold concentrations for industrial land use.

Unlike conventional mineral processing, where flotation performance is generally evaluated based on concentrate grade and metal recovery, the present investigation adopted a broader set of performance indicators reflecting the objectives of environmental remediation. Particular emphasis was placed on maximising the recovery of sediments potentially suitable for beneficial reuse while minimising the generation of highly contaminated residues requiring disposal.

The experimental results demonstrate that the proposed treatment strategy can achieve these objectives over a wide range of sediment characteristics. Although treatment performance varied among the investigated process configurations, the integrated flowsheet consistently reduced contaminant concentrations while concentrating most of the contaminant load into a comparatively small residual fraction.

The following sections discuss the experimental results in terms of overall treatment performance, contaminant removal, process selectivity and the influence of the different treatment configurations on the effectiveness of the proposed remediation strategy.

3.3.1. Overall Treatment Performance

The overall results obtained for the five treatment tests are summarised in Table 9, which reports contaminant concentrations, mass yields (Y) for both individual flotation products and the final decontaminated and non-decontaminated fractions, metal recoveries (ϱi) and removal efficiencies (REi) for all process products.

Table 9. Overall performance of the five laboratory-scale treatment configurations, including contaminant concentrations (in mg kg^{-1}), product masses (*W* in g), mass yields of flotation products (Y_P, dimensionless), mass yields of final products (Y_F, dimensionless) metal recoveries (ρ_i, dimensionless) and removal efficiencies (*REi*, dimensionless) for the different process products. (NH = Natural Hydrophobic). Values represent the mean of two independent flotation runs (n = 2).

	Products	Zn	ϱZn	Pb	ϱPb	Cd	ϱCd	Hg	ϱHg	W	Yp	YF	Σ ϱi
BE4_0.0-0.2b	NH froth	5459	0.04	2001	0.07	43	0.05	33.2	0.09	11.90	0.03		0.24
	+250 µm	734	0.01	458	0.02	6	0.01	4.3	0.02	15.98	0.04		0.05
	−20 µm	11,034	0.21	2756	0.25	92	0.25	38.6	0.26	30.66	0.08		0.97
	Sulphide froth	58,788	0.32	2306	0.06	379	0.30	39.7	0.08	8.93	0.02		0.76
	Oxides froth	10794	0.09	1986	0.08	52	0.06	24.0	0.07	13.00	0.03		0.29
	Tailings	1767	0.34	589	0.53	11.90	0.33	7.1	0.49	308.90	0.79		1.68
	DP	1716		583		11.61		7.0		324.88		0.83	1.73
	NDP	16,569		2399		115		34.8		64.49		0.17	2.26
	F	4176	1.00	883	1.00	28.68	1.00	11.6	1.00	389.40	1.00	1.00	
	REi [-]	0.66		0.45		0.66		0.50					
BE4_0.0-0.2c	NH froth	6324	0.10	2116	0.13	59	0.14	45.93	0.21	22.21	0.06		0.58
	Sulphide froth	32,521	0.38	2834	0.12	223	0.38	101.81	0.33	15.72	0.04		1.20
	+250 µm	711	0.01	519	0.03	6.18	0.01	2.25	0.01	20.90	0.05		0.06
	−20 µm	5810	0.09	4076	0.23	46	0.10	24.57	0.10	20.19	0.05		0.52
	Oxides froth	6750	0.13	1216	0.09	44	0.12	11.52	0.06	25.89	0.07		0.40
	Tailings	1414	0.30	515	0.41	8.03	0.25	4.86	0.29	285.85	0.73		1.23
	DP	1366		515		7.90		4.68		306.75		0.79	1.30
	NDP	11,234		2444		82		41		84.01		0.21	2.70
	F	3488	1.00	930	1.00	23.81	1.00	12.41	1.00	390.76	1.00	1.00	
	REi [-]	0.69		0.57		0.74		0.70					
BE4_comp	NH froth	5663	0.07	2927	0.10	67	0.10	79.61	0.21	15.31	0.04		0.48
	+250 µm	317	0.01	502	0.03	3.34	0.01	1.18	0.01	25.52	0.07		0.05
	Sulphide froth	32,712	0.46	5087	0.20	288	0.50	152.61	0.46	17.38	0.04		1.61
	−20 µm	7328	0.12	4038	0.19	70	0.15	31.00	0.11	20.87	0.05		0.57
	Oxides froth	3491	0.13	1927	0.19	21	0.09	7.37	0.06	44.76	0.12		0.47
	Tailings	968	0.21	495	0.29	5.77	0.15	3.54	0.16	264.81	0.68		0.81
	DP	910		496		5.56		3.33		290.33		0.75	0.86
	NDP	9809		3089		86		49		98.32		0.25	3.14
	F	3162	1.00	1152	1.00	25.88	1.00	14.96	1.00	388.65	1.00	1.00	
	REi [-]	0.79		0.68		0.84		0.83					

BE5_0.2-1.0b	NH froth	5097	0.05	2563	0.07	65	0.08	146	0.22	7.54	0.02		0.42
	+250 μm	264	0.02	226	0.05	1.73	0.02	1.27	0.01	57.62	0.15		0.10
	Sulphide froth	29,320	0.40	4410	0.16	255	0.44	231	0.47	10.19	0.03		1.46
	−20 μm	8358	0.14	4938	0.23	87	0.19	54	0.14	12.70	0.03		0.69
	Oxides froth	5487	0.23	2443	0.28	37	0.20	7.02	0.04	31.77	0.08		0.76
	Tailings	442	0.16	200	0.20	1.71	0.08	2.20	0.12	277.14	0.70		0.57
	DP	412		205		1.71		2.04		334.76		0.84	0.67
	NDP	9930		3289		87		70		62.20		0.16	3.33
	F	1903	1.00	688	1.00	15	1.00	12.7	1.00	396.96	1.00	1.00	
	REi [-]	0.82		0.75		0.90		0.87					
BE6_0.2-1.0b	NH froth	8416	0.09	4841	0.14	106	0.12	109.66	0.30	18.83	0.05		0.65
	+250 μm	371	0.02	283	0.03	5.18	0.03	1.17	0.01	80.73	0.21		0.09
	Sulphide froth	102,437	0.47	16,569	0.19	997	0.49	208.45	0.24	7.82	0.02		1.39
	−20 μm	9738	0.14	6735	0.25	104	0.16	71.79	0.26	24.58	0.06		0.80
	Oxides froth	4215	0.09	2110	0.12	31	0.07	16.50	0.09	37.83	0.10		0.38
	Tailings	1390	0.18	826	0.27	9.06	0.13	3.22	0.10	223.87	0.57		0.69
	DP	1121		682		8.03		2.68		304.6		0.77	0.78
	NDP	15,252		5233		152		68		89.06		0.23	3.22
	F	4318	1.00	1712	1.00	40.60	1.00	17.53	1.00	393.66	1.00	1.00	
	REi [-]	0.80		0.69		0.85		0.88					
	CTC_B	1500		1000		15		5					

The experimental programme followed a two-step approach. Three alternative flowsheet configurations (BE4_0.0–0.2b, BE4_0.0–0.2c and BE4_comp) were first evaluated using sediment samples belonging to the Cluster I, to minimise differences in feed characteristics during the comparative assessment. In particular, BE4_0.0–0.2b and BE4_0.0–0.2c were tested on aliquots of the same homogenised sample, whereas BE4_comp was tested on a composite sample from the same sampling cell. Based on the results of this comparison, the best-performing flowsheet among those investigated, corresponding to BE4_comp, was selected and subsequently applied to BE5_0.2–1.0b and BE6_0.2–1.0b, representing Clusters II and III, respectively.

The investigated treatment tests consistently produced two final products characterised by markedly different contaminant concentrations. The decontaminated product (DP) complied with the CTC_B and met one of the chemical prerequisites relevant for its potential terrestrial reuse, whereas the non-decontaminated product (NDP) contained the contaminant-enriched fractions requiring further management or disposal. Despite the substantial variability in the initial contaminant concentrations among the sediment samples, four of the five treatment tests successfully reduced the concentrations of all target contaminants below the corresponding CTC_B values in the final DP. The only exception was BE4_0.0–0.2b, in which the final Zn (1716 mg/kg) and Hg (7 mg/kg) concentrations remained slightly above the corresponding CTC_B values of 1500 mg/kg and 5 mg/kg.

Zn, Cd and Hg generally showed the highest removal efficiencies, whereas Pb removal was comparatively lower. Within the comparative phase, BE4_comp showed the highest overall contaminant-removal efficiencies among the three alternative flowsheet configurations. The same flowsheet, when subsequently applied to BE5_0.2–1.0b and BE6_0.2–1.0b, also achieved high removal efficiencies, with Zn, Cd and Hg generally exceeding 70%–80%, while Pb removal was lower but still sufficient to satisfy the remediation objectives.

An important outcome of the experimental programme is that compliance with the regulatory limits was achieved while maintaining a relatively high recovery of treated sediment. Depending on the treatment test, approximately 75%–85% of the treated

material was recovered as DP, whereas only 15%–25% of the initial sediment mass was concentrated into the NDP. This represents a favourable compromise between remediation efficiency and waste minimisation, one of the principal objectives of sediment treatment.

Overall, the results confirm that the proposed integrated treatment process can reduce the concentrations of target contaminants below the CTC_B values established by Italian legislation for industrial land use, while substantially reducing the volume of contaminated material requiring disposal. These findings provide the basis for the more detailed evaluation of contaminant removal and process selectivity presented in the following sections.

3.3.2. Contaminant Removal

The contaminant removal achieved by the integrated treatment process is summarised in Figure 11, which compares the contaminant concentrations in the feed (F), the decontaminated product (DP) and the non-decontaminated product (NDP), normalised to the corresponding CTC_B values.

Normalisation of the analytical results to the corresponding CTC_B values provides a direct assessment of the remediation objectives, allowing contaminants characterised by different regulatory thresholds to be compared on the same basis.

Following treatment, the contaminant concentrations in the DP decrease substantially for all investigated tests. As discussed in Section 3.3.1, four of the five experimental tests reduced the concentrations of Zn, Pb, Cd and Hg below the corresponding CTC_B values. Figure 11 further highlights the marked partitioning of the contaminant load between the two final products, with the NDP consistently showing substantially higher normalised contaminant concentrations than the corresponding DP.

Within the three BE4 tests (Cluster I), Figure 11 shows a progressive improvement in contaminant separation. In BE4_0.0–0.2b, Zn and Hg remained 14% and 40.0% above their respective CTC_B values in the DP, whereas Pb and Cd were already 41.7% and 22.6% below the corresponding thresholds. In BE4_0.0–0.2c, all four contaminants complied with the regulatory limits, with Zn, Pb, Cd and Hg concentrations 9%, 48%, 47% and 6% below their respective CTC_B values. A further improvement was observed in BE4_comp, where the corresponding concentrations were 39%, 50%, 60% and 32% below the CTC_B values. At the same time, the NDP was strongly enriched in contaminants: in BE4_comp, Zn, Pb, Cd and Hg reached approximately 6.5, 3.1, 5.7 and 9.8 times their respective CTC_B values. Thus, the progression from BE4_0.0–0.2b to BE4_comp involved not only achievement of regulatory compliance in the DP but also increasingly effective partitioning of the contaminant load towards the NDP.

Comparison of BE4_0.0–0.2b, BE4_0.0–0.2c and BE4_comp shows a progressive improvement in overall contaminant removal across the investigated tests, associated with different arrangements of the particle-size classification stages. BE4_0.0–0.2b, in which both classification stages were performed upstream of sulphide flotation, showed the lowest removal efficiencies. In BE4_0.0–0.2c, the fine fraction was retained during sulphide flotation, and was associated with higher removal efficiencies. Since these two configurations were tested using aliquots of the same homogenised sediment sample, their comparison provides more direct evidence of the influence of flowsheet arrangement on treatment performance. The best overall performance within the comparative phase was obtained for BE4_comp, in which the +250 μm fraction was removed before sulphide flotation, whereas the −20 μm fraction was retained during this stage and removed only before the subsequent flotation of oxidised minerals. This configuration was therefore identified as the best-performing among the investigated tests.

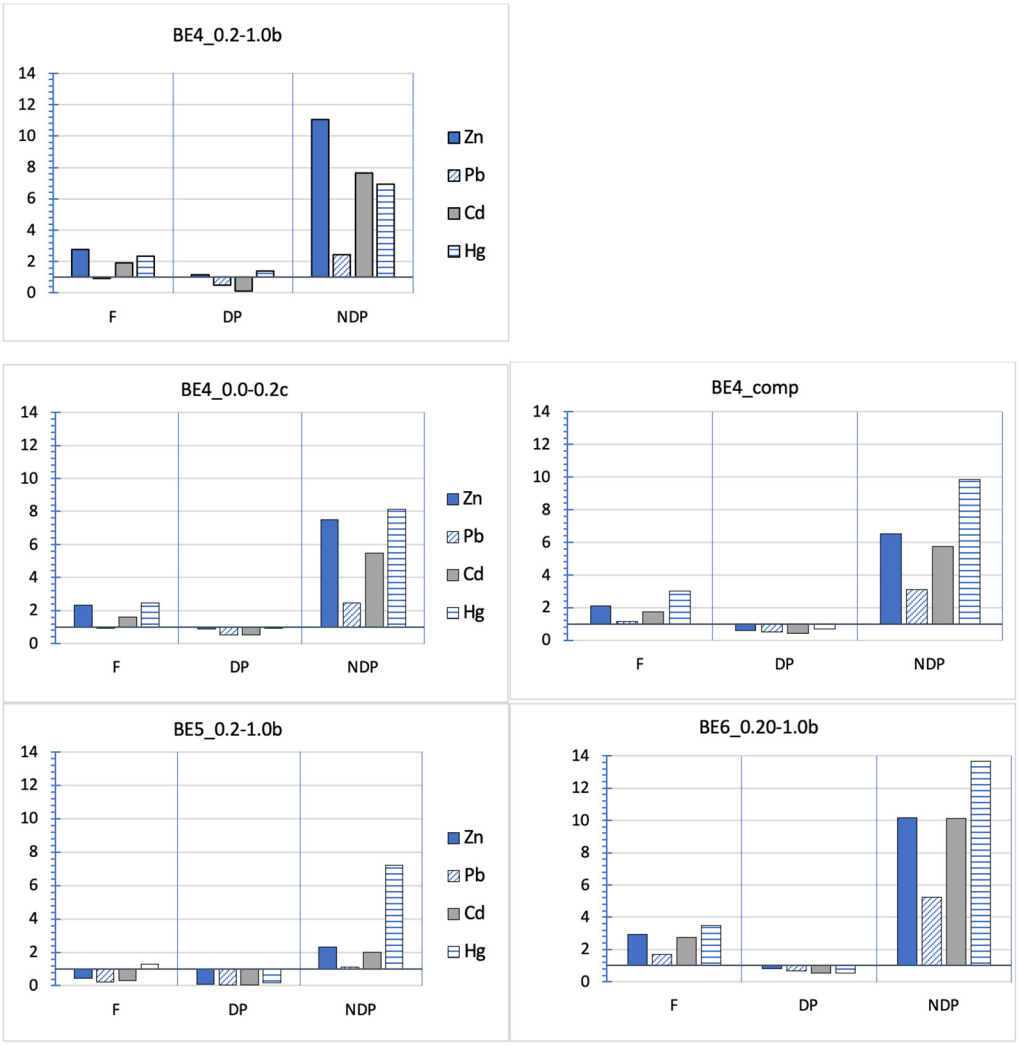


Figure 11. Normalised contaminant concentrations (C/CTCB) in the feed (F), decontaminated product (DP) and non-decontaminated product (NDP) obtained for the five investigated treatment configurations. The horizontal axis is drawn at C/CTCB = 1 to highlight exceedances of the regulatory threshold.

This arrangement is consistent with the particle-size characteristics of the investigated sediments. The improved treatment performance observed when the fine fraction was retained during sulphide flotation suggests that the presence of fines during this stage may have contributed to the observed separation behaviour.

The beneficial effect observed when retaining the fine fraction during sulphide flotation is also consistent with previous studies showing that moderate amounts of fine particles can influence froth behaviour and enhance flotation performance [65–69].

The preliminary removal of the +250 μm fraction is consistent with the sediment characterisation results, which showed that this coarse fraction already complied with the CTC_B values for all target contaminants. Its separation before sulphide flotation therefore prevents an already compliant sediment fraction from unnecessarily entering the flotation circuit. This arrangement may also be favourable from a flotation perspective, since coarse particles are generally more susceptible to bubble–particle detachment and consequently show decreasing recovery in conventional mechanical flotation cells as particle size increases [70,71].

The subsequent removal of the residual −20 μm fraction before oxidised-mineral flotation may therefore represent a favourable compromise between the requirements of the

two flotation stages. Fines removal before oxidised-mineral flotation is consistent with the specific requirements of the sulfidisation–amine route used for Zn oxide recovery.

Zn oxide flotation following Na_2S sulfidisation and amine addition is particularly sensitive to the presence of slimes, and desliming has been identified as an important factor controlling both Zn recovery and concentrate quality [72]. Excessive fine-particle contents can increase reagent consumption and promote slime coating of mineral surfaces, thereby hindering collector adsorption and subsequent bubble–particle attachment. This mechanism may be particularly relevant to the investigated sediments because quartz represents one of the main gangue minerals, and quartz slime coating has specifically been reported to impair Zn oxide flotation under sulfidisation–amine conditions. Thus, positioning the −20 μm classification between sulphide and oxidised-mineral flotation may allow the potential benefits of retaining fines during sulphide flotation to be exploited while limiting their detrimental effects on the subsequent Na_2S–amine flotation stage.

Taken together, the comparison among BE4_0.0–0.2b, BE4_0.0–0.2c and BE4_comp indicates that treatment performance may depend not only by the presence or absence of particle-size classification, but also by the position of the two classification stages relative to the flotation stages. Within this comparative phase, BE4_comp provided the most favourable overall contaminant-removal performance among the investigated configuration and was therefore selected for subsequent application to the other sediment groups.

The selected flowsheet remained effective when subsequently applied to BE5_0.2–1.0b (Cluster II) and BE6_0.2–1.0b (Cluster III) despite their different feed characteristics. Removal efficiencies reached 82%, 75%, 90% and 87% for Zn, Pb, Cd and Hg, respectively, in BE5_0.2–1.0b, and 79%, 69%, 85% and 88%, respectively, in BE6_0.2–1.0b.

Figure 11 provides further evidence of the performance of the selected flowsheet under these different feed conditions. In BE5_0.2–1.0b, the final DP concentrations of Zn, Pb, Cd and Hg were 71%, 80%, 89% and 56% below their respective CTC_B values. Despite the substantially higher initial contamination of BE6_0.2–1.0b, the corresponding DP concentrations remained 19%, 32%, 47% and 46% below the regulatory thresholds. At the same time, strong contaminant enrichment was observed in the corresponding NDP. This was particularly evident for BE6_0.2–1.0b, where Zn, Pb, Cd and Hg reached approximately 10.2, 5.2, 10.1 and 13.6 times their respective CTC_B values.

The behaviour of BE6_0.2–1.0b is particularly relevant because it represents the most heavily contaminated sediment investigated. Its feed contained Zn, Pb, Cd and Hg at approximately 2.9, 1.7, 2.7 and 3.5 times their respective CTC_B values; nevertheless, treatment produced a DP in which all four contaminants complied with the regulatory thresholds. The simultaneous decrease in contaminant concentrations in the DP and their strong enrichment in the NDP indicates that the selected flowsheet maintained effective contaminant partitioning even under the highest contamination conditions investigated.

An important finding is that differences in the initial particle-size distributions did not necessarily correspond to poorer overall remediation performance. In particular, BE5_0.2–1.0 and BE6_0.2–1.0 exhibited coarser particle-size distributions than BE4_0.0–0.2, with d_{80} values of approximately 232 and 283 μm, respectively, compared with 173 μm for BE4_0.0–0.2. Despite their coarser particle-size distributions, the selected treatment configuration achieved high contaminant-removal efficiencies and produced decontaminated sediments complying with the investigated regulatory thresholds. These findings suggest that the initial particle-size distribution alone is insufficient to predict the overall effectiveness of the integrated remediation process. In this context, the incorporation of particle-size classification within the flotation circuit may have contributed to mitigating the influence of feed granulometry by separating the coarser fraction before sulphide flotation and removing the residual ultrafine fraction before oxidised-mineral flotation.

In particular, the results indicate that contaminant removal depends not only on the efficiency of the individual separation stages, but also on the sequence in which particle-size classification and flotation are integrated within the treatment flowsheet. This interpretation is consistent with both the experimental trends and the particle-size effects reported in flotation literature.

Moreover, the performance achieved for configuration BE6_0.2–1.0b indicates that the proposed flowsheet remained effective for the most heavily contaminated sediment investigated, despite its substantially higher initial contaminant concentrations. This suggests that the selected sequence of classification and flotation stages was effective across the range of contamination levels investigated in this study, although its applicability beyond these sediments would require further validation.

3.3.3. Mass Distribution and Process Selectivity

The effectiveness of the proposed remediation process depends not only on contaminant removal but also on the distribution of sediment mass between the DP and the NDP. In this context, process selectivity is defined as the ability to recover the largest possible sediment mass complying with the CTC_B values while transferring the contaminant inventory to the smallest possible residual stream.

The mass distributions obtained for the five investigated treatment configurations are summarised in Figure 12.

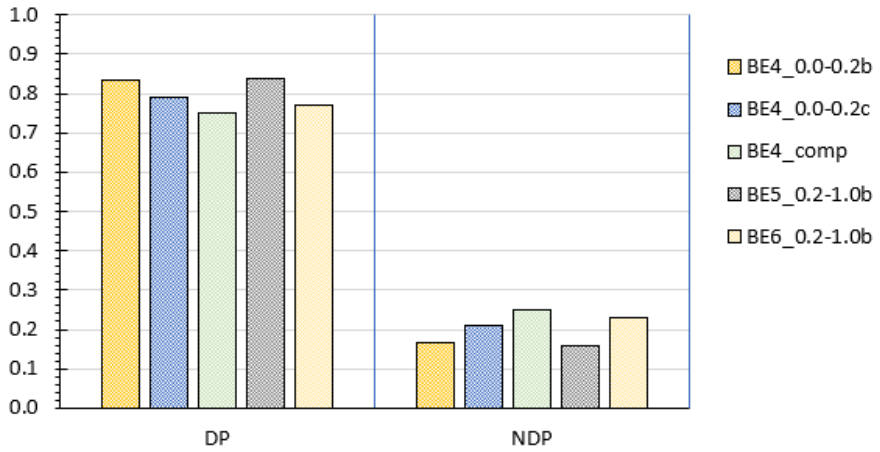


Figure 12. Mass distribution between the decontaminated product (DP) and the non-decontaminated product (NDP) for the five investigated treatment tests.

For all investigated tests, the integrated treatment process successfully concentrated a substantial proportion of the contaminant load into a relatively small mass fraction. Depending on the adopted process conditions, approximately 75%–85% of the treated sediment was recovered as DP, whereas only 15%–25% was transferred to the NDP. Importantly, four of the five investigated tests combined this high sediment recovery with concentrations of all target contaminants below the corresponding CTC_B values in the DP. When Figures 11 and 12 are considered together, the effectiveness of the treatment therefore becomes more evident, as regulatory compliance was generally achieved without transferring a large proportion of the treated sediment to the NDP.

The mass distribution did not exactly follow the same trend observed for contaminant removal, confirming that sediment recovery and contaminant removal represent complementary rather than interchangeable indicators of process performance. Notably, BE5_0.2–1.0b combined the highest DP mass recovery (about 84%) with the high contaminant-removal efficiencies discussed in Section 3.3.2. In contrast, BE4_0.0–0.2b also

achieved a high DP recovery (approximately 83%), but the resulting product remained above the CTC_B values for Zn and Hg. These results demonstrate that maximising the recovered sediment mass alone does not necessarily correspond to optimal process performance, since the quality of the recovered product must be considered simultaneously.

This distinction is particularly relevant when comparing BE4_0.0–0.2c with the last three configurations. BE4_0.0–0.2c recovered approximately 79% of the initial sediment mass as a compliant DP and therefore also represents an effective treatment configuration in terms of mass recovery. However, as discussed in Section 3.3.2, BE4_comp, BE5_0.2–1.0b and BE6_0.2–1.0b achieved higher contaminant-removal efficiencies. Accordingly, the improved performance associated with the last three configurations should not be interpreted as a systematic increase in DP mass recovery, but rather as a more effective contaminant partitioning while maintaining a substantial proportion of the sediment in the decontaminated stream.

The relatively small mass of the NDP was accompanied by a pronounced enrichment in contaminants compared with the corresponding DP, demonstrating that the treatment transferred contaminants to a comparatively limited residual stream. For example, in BE4_0.0–0.2c, approximately 79% of the initial sediment mass was recovered as DP, containing 1366 mg/kg Zn, 515 mg/kg Pb, 7.90 mg/kg Cd and 4.68 mg/kg Hg, whereas the NDP represented only approximately 21% of the initial mass but contained 11,234 mg/kg Zn, 2444 mg/kg Pb, 82 mg/kg Cd and 41 mg/kg Hg. Thus, the reduction in contaminant concentrations in the DP was accompanied by their effective concentration into a substantially smaller residual mass.

Process selectivity can therefore be interpreted as the combined outcome of contaminant enrichment and mass partitioning. Excessive recovery of floated material may increase contaminant removal but simultaneously enlarges the quantity of material requiring further treatment or controlled management, thereby reducing the overall economic and environmental efficiency of the treatment process. Conversely, maximising DP recovery is advantageous only when contaminant concentrations remain below the target thresholds. The optimal treatment configuration should therefore achieve a balance between these competing requirements, and process selectivity should be evaluated by considering contaminant partitioning and sediment recovery simultaneously rather than as independent performance indicators.

The present results demonstrate that the proposed integrated treatment strategy successfully reconciles these objectives. By combining particle-size classification with sequential flotation stages, the process concentrates contaminants into a limited residual fraction while preserving at least approximately three-quarters of the initial sediment mass as DP in all investigated tests. More importantly, four tests achieved this mass recovery while simultaneously reducing all target contaminant concentrations below the corresponding CTC_B values. The selected flowsheet maintained this balance when applied to sediments with different characteristics, with BE5_0.2–1.0b providing the most favourable combination of DP mass recovery and contaminant removal among the five treatment tests.

This balance is consistent with the rationale of physical and physicochemical remediation approaches reported for contaminated soils and sediments, in which treatment effectiveness depends on selectively concentrating contaminants into a reduced mass fraction while maximising the recovery of less-contaminated material [26,28,49].

From a process engineering perspective, these findings emphasise that optimisation should focus on the performance of the integrated treatment flowsheet rather than on the efficiency of individual unit operations. The overall selectivity of the process results from the interaction between particle-size classification, flotation and product management, highlighting the importance of flowsheet design in achieving effective sediment remediation.

3.3.4. Contribution of Individual Process Stages

Although the overall treatment performance is ultimately determined by the integrated behaviour of the entire flowsheet, the contribution of the individual unit operations provides valuable insight into the mechanisms governing contaminant removal. The removal efficiencies associated with the different process stages are summarised in Figure 13.

The results indicate that contaminant removal is not uniformly distributed among the different unit operations. Instead, each process stage contributes according to the mineralogical occurrence, particle-size distribution and flotation behaviour of the contaminant-bearing phases.

Flotation of the naturally hydrophobic material removed a comparatively small proportion of the total sediment mass but, in some tests, contributed appreciably to contaminant removal. This behaviour indicates that contaminants were partly associated with naturally floatable material or were transferred to this product through non-selective mechanisms such as entrainment.

Among the investigated unit operations, sulphide flotation provides the greatest contribution to the overall heavy metals removal. This behaviour is consistent with the mineralogical characterisation presented in Section 3.1.2, which demonstrated that part of the contaminants is associated with sulphide minerals exhibiting favourable flotation properties. Consequently, sulphide flotation represents the key separation stage within the proposed remediation process.

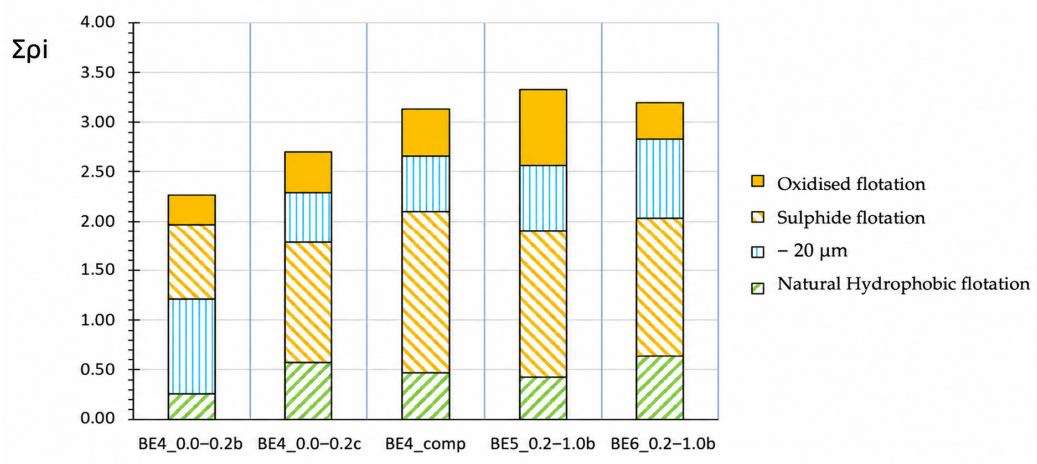


Figure 13. Cumulative contaminant removal contribution (Σρi) associated with the individual unit operations for the five investigated treatment tests.

The contribution of the −20 µm particle-size classification varies according to the investigated sediment and treatment configuration but becomes particularly significant when applied immediately before the flotation of the oxidised fraction. Besides removing a highly contaminated fine fraction, this operation may also favours flotation selectivity by limiting the detrimental effects, reported in the literature, of slimes on bubble–particle interactions, as discussed in Section 1.2.

The oxidised flotation stage provides an additional, although generally smaller, contribution to contaminant removal. Its importance depends on the proportion of contaminants occurring in oxidised mineral forms and therefore varies among the investigated sediments. Nevertheless, the results demonstrate that this stage contributes to achieving compliance with the remediation objectives, particularly for the configurations yielding the highest overall treatment efficiencies.

By contrast, the preliminary removal of the +250 μm fraction contributes only marginally to direct contaminant removal because this fraction already exhibits relatively low contaminant concentrations. Its principal role within the treatment flowsheet is therefore not to remove contaminants directly but to reduce the mass requiring flotation.

The relative contributions of the individual process stages confirm that the observed treatment performance results from their complementary functions rather than from a single separation mechanism. Sulphide flotation provides the main contribution to contaminant removal, particle-size classification selectively excludes fractions that either require no further treatment or may adversely affect subsequent flotation, and oxidised-mineral flotation provides an additional removal step for the contaminant inventory remaining after sulphide flotation. From a process-engineering perspective, the results therefore indicate that treatment effectiveness is governed by the sequence and interaction of the individual operations within the integrated flowsheet. In particular, the comparative BE4 tests suggest that the position of the two particle-size classification stages represent an important key design variable, while the application of the selected configuration to BE5_0.2–1.0b and BE6_0.2–1.0b demonstrates that the resulting flowsheet can maintain high contaminant removal and substantial sediment recovery under different feed conditions.

3.3.5. Physicochemical Interpretation of Flotation Performance

The differences in contaminant removal observed among the investigated treatment tests can be interpreted considering the interactions between mineral surface properties, flotation reagents and particle-size distribution. In particular, particle–bubble attachment depends on the hydrophobicity of mineral surfaces, which can be modified through reagent adsorption and surface chemical reactions, whereas particle size influences collision and detachment probabilities [41,42,73,74]. These mechanisms provide a basis for interpreting the different responses of the contaminant-bearing particles during the sequential flotation stages.

During the initial collector-free flotation stage, Dowfroth 1012 promoted bubble formation and froth stability [75]. The recovery of naturally floatable particles, together with possible mechanical entrainment, may explain the transfer of contaminants into this product. This behaviour was particularly evident for Hg in BE5_0.2–1.0b and BE6_0.2–1.0b, where approximately 22% and 30% of the initial Hg inventory, respectively, were recovered in a relatively small froth fraction.

The major contribution of sulphide flotation to Zn and Cd removal is consistent with the mineralogical identification of sulphide phases in the flotation concentrate. The addition of $CuSO_4$ promotes sphalerite activation, favouring xanthate adsorption and increasing surface hydrophobicity, thereby facilitating particle–bubble attachment [76]. For instance, in BE6_0.2–1.0b, approximately 47% of Zn and 49% of Cd were recovered in the sulphide froth, which represented only about 2% of the initial sediment mass. The similar behaviour of Zn and Cd may reflect their association with common contaminant-bearing mineral phases. Conversely, the generally lower Pb recovery suggests differences in mineralogical association, surface response or liberation characteristics that cannot be resolved from the available analyses.

The contribution of the final flotation stage can be interpreted considering the surface modification mechanisms associated with Na_2S and amine collectors. Previous studies have demonstrated that sulphidisation can favour amine adsorption and improve the floatability of oxidised zinc minerals [64,77,78].

Particle-size effects provide a further possible explanation for the differences among the BE4 treatment configurations. Although ultrafine particles may reduce flotation selectivity through low collision efficiency, slime coating and entrainment, previous studies

have also demonstrated that moderate fine-particle contents can influence froth stability and flotation recovery [67,69]. In the present study, retaining the −20 μm fraction during sulphide flotation was associated with increased Zn, Cd and particularly Hg recovery. For example, Hg recovery in the sulphide froth increased from approximately 8% in BE4_0.0–0.2b to 33% in BE4_0.0–0.2c. This behaviour is consistent with a possible contribution of fine particles to froth behaviour and particle transport, although differences between the feed samples and other process-related factors prevent a direct causal interpretation.

The effectiveness of the selected flowsheet on the coarser BE5 and BE6 sediments can also be related to the distribution of contaminants among particle-size fractions. In BE6_0.2–1.0b, the +250 μm fraction represented approximately 21% of the sediment mass but contained only 1%–3% of the initial contaminant inventories, whereas the −20 μm fraction accounted for approximately 6% of the mass and 14%–26% of the contaminants. Consequently, particle-size classification allowed substantial mass separation while selectively directing contaminant-bearing fractions towards the NDP. This contributed to the overall remediation performance without requiring the flotation of the entire sediment feed.

Overall, the experimental results are consistent with the combined influence of mineral surface chemistry, particle-size distribution and the arrangement of the treatment stages. However, future investigations could further explore the underlying flotation mechanisms through direct measurements of surface hydrophobicity, collector adsorption and particle–bubble interactions.

3.4. Process Optimisation and Implication for Sediment Remediation

The experimental programme demonstrates that the optimisation of sediment remediation by flotation should be approached as a flowsheet design problem rather than as the optimisation of individual flotation stages. The overall performance of the proposed treatment process is governed by the interaction among particle-size classification, sequential flotation, reagent scheme and product management, all of which contribute to achieving the remediation objectives. Within the investigated experimental conditions, the comparative assessment enabled the identification of the best-performing flowsheet, based on the combined evaluation of contaminant removal, regulatory compliance and sediment recovery.

The sediment characterisation programme proved to be an essential preliminary step in process design. Particle-size distribution, mineralogical composition and geochemical partitioning collectively provided the information required to identify the most appropriate sequence of unit operations. In particular, the occurrence of sulphide phases, together with their preferential association with the finer particle-size fractions, justified the adoption of a treatment strategy integrating particle-size classification with sequential sulphide and oxidised flotation.

An important implication of the present study is that remediation performance should not be evaluated solely in terms of contaminant removal efficiency or metal recovery. Instead, optimisation should consider the simultaneous achievement of three complementary objectives: (i) compliance with the CTC_B, (ii) maximisation of the mass of sediment potentially suitable for beneficial reuse, and (iii) minimisation of the quantity of contaminant-enriched material requiring controlled disposal.

From an environmental engineering perspective, the most significant outcome is not the absolute magnitude of contaminant removal, but the achievement of regulatory compliance. The experimental results show that the proposed process can produce a large sediment fraction complying with the target CTC_B values, while concentrating the contaminant load into a smaller residual stream requiring controlled management. Compliance with CTC_B represents an important prerequisite for potential beneficial reuse,

although actual reuse would require assessment against the additional technical and environmental requirements applicable to the intended reuse scenario.

This multi-objective process evaluation is consistent with the current evolution of flotation-based remediation technologies towards integrated treatment strategies rather than optimisation of individual separation stages [79].

Although the proposed treatment process was specifically developed for the contaminated sediments of the Portovesme industrial harbour, the design methodology adopted in this study is potentially applicable to other contaminated marine sediments exhibiting comparable mineralogical, granulometric and geochemical characteristics. In particular, the integration of sediment characterisation with process design provides a rational framework for selecting the most appropriate sequence of unit operations according to the characteristics of the contaminated material rather than adopting a standard treatment scheme.

The present results also highlight the importance of combining mineral processing principles with environmental engineering criteria. Rather than adapting conventional flotation circuits without modification, remediation processes should be specifically designed according to the environmental objectives to be achieved. In this respect, the present laboratory-scale results show that technologies traditionally developed for ore beneficiation can be effectively adapted to the treatment of contaminated sediments when integrated within a flowsheet specifically designed according to environmental remediation objectives

4. Conclusions

The results demonstrate that flotation, when integrated with particle-size classification, can provide an effective remediation strategy for marine sediments contaminated by mining and metallurgical wastes. Sediment characterisation showed that contaminant occurrence is primarily controlled by mineralogical association and particle-size distribution, thereby providing the basis for the proposed treatment flowsheet.

The laboratory-scale experimental programme showed that the proposed integrated process can reduce contaminant concentrations below the contamination threshold concentrations established by Italian legislation for industrial land use (CTC_B) in four of the five investigated treatment tests. Approximately 75%–85% of the treated sediment was recovered as decontaminated product, while contaminants were concentrated into a relatively small residual fraction, substantially reducing the quantity of material requiring controlled disposal. Removal efficiencies reached up to approximately 75% for Pb, 82% for Zn and close to 90% for Cd and Hg.

One of the main findings of this study is that remediation performance is governed by the overall flowsheet configuration and by the interaction between particle-size classification and sequential flotation, rather than by the performance of individual flotation stages alone. Within the comparative BE4 tests, differences in the position of the classification stages relative to sulphide and oxidised-mineral were associated with differences in the final contaminant partitioning. Among the investigated configurations, the most favourable performance was obtained when the +250 μm fraction was removed before sulphide flotation, while the −20 μm fraction was retained during this stage and removed before the subsequent flotation of oxidised minerals. This configuration was identified as the best-performing among those investigated, based on the combined evaluation of regulatory compliance, sediment recovery and contaminant concentration in the residual fraction and was subsequently successfully applied to sediments with different feed characteristics.

The present results also indicate that flotation-based remediation should be evaluated according to environmental performance criteria rather than conventional mineral

processing indicators alone. Regulatory compliance, recovery of sediments meeting the investigated chemical criteria relevant to potential beneficial reuse and minimisation of the contaminant-enriched fraction should therefore be considered complementary optimisation objectives.

Although the proposed treatment strategy was developed for the Portovesme sediments, the methodology adopted in this study may serve as a general framework for designing flotation-based remediation processes for contaminated marine sediments exhibiting similar mineralogical and geochemical characteristics. Future research should address pilot-scale validation, including process economics, water and reagent consumption, process-water recycling, dewatering of the final products and management of the contaminant-enriched NDP.

Author Contributions: Conceptualization, P.B., P.M., G.S. and B.G.; methodology, P.B., P.M. and G.S.; investigation, P.M., P.B. and G.S.; data curation, P.M., G.S., F.P. and A.L.; writing—original draft preparation, P.M., G.S., F.P. and A.L.; writing—review and editing, G.S., F.P., A.L. and V.D.; supervision, P.B., P.M., B.G. and V.D. All authors have read and agreed to the published version of the manuscript.

Funding: This research received no external funding.

Data Availability Statement: The data presented in this study are available on request from the corresponding author.

Acknowledgments: Research carried out in the framework of projects conducted by CESA (Centre of excellence on environmental sustainability, Sardinia, Italy) and CINIGeo (National Interuniversity Consortium for Geo-resources Engineering between the University of Bologna, Cagliari, Rome "La Sapienza" and Trieste, Italy).

Conflicts of Interest: The authors declare no conflicts of interest.

References

1. Dorleon, G.; Rigaud, S.; Techer, I. Management of dredged marine sediments in Southern France: Main keys to large-scale beneficial re-use. *Environ. Sci. Pollut. Res.* **2024**, *32*, 16656–16679. https://doi.org/10.1007/s11356-024-33129-9.
2. Carreira, C.; Bollwerk, S.M.; Lønborg, C. A review on beneficial use of dredged marine sediment. *Anthr. Coasts* **2025**, *8*, 12. https://doi.org/10.1007/s44218-025-00076-y.
3. Fratini, C.; Anselmi, S.; Renzi, M. Dredge Sediment as an Opportunity: A Comprehensive and Updated Review of Beneficial Uses in Marine, River, and Lagoon Eco-Systems. *Environments* **2024**, *12*, 200. https://doi.org/10.3390/environments12060200.
4. Malarbì, D.; Falciglia, P.P.; Vagliasindi, F.G.A. Removal of Hg from Real Polluted Sediments Using Enhanced-EK Decontamination: Verification of Experimental Methods and Batch-Test Preliminary Results. *J. Chem.* **2015**, *2015*, 270451. https://doi.org/10.1155/2015/270451.
5. Zhang, Y.; Labianca, C.; Chen, L.; De Gisi, S.; Notarnicola, M.; Guo, B.; Sun, J.; Ding, S.; Wang, L. Sustainable ex-situ remediation of contaminated sediment: A review. *Environ. Pollut.* **2021**, *287*, 117333. https://doi.org/10.1016/j.envpol.2021.117333.
6. Welsch, M.; Bentsen, S.; Henning, M. Focused review of recent advances of sediment treatment technologies. *Integr. Environ. Assess. Manag.* **2025**, *21*, 986–999. https://doi.org/10.1093/inteam/vjaf046.
7. Careghini, A.; Dastoli, S.; Ferrari, G.; Saponaro, S.; Bonomo, L.; De Propris, L.; Gabellini, M. Sequential solidification/stabilization and thermal process under vacuum for the treatment of mercury in sediments. *J. Soils Sediments* **2010**, *10*, 1646–1656. https://doi.org/10.1007/s11368-010-0290-7.
8. Xu, Q.; Wu, B.; Chai, X. In Situ Remediation Technology for Heavy Metal Contaminated Sediment: A Review. *Int. J. Environ. Res. Public Health* **2022**, *19*, 16767. https://doi.org/10.3390/ijerph192416767.
9. Sogos, G.; Pinna, F.; De Gioannis, G.; Lai, A.; Dentoni, V.; Serpe, A.; Muntoni, A.; Grosso, B. Evaluation of the Ecological and Health Risk Associated with Abandoned Tailings Storage Facilities: The Case of Montevecchio Levante (Sardinia, Italy). *Processes* **2025**, *13*, 2629. https://doi.org/10.3390/pr13082629.

10. Swetha, S.; Veerasingam, S.; Rajendran, S.; Hassan, H.; Hashmi, M.Z.U.R.R.; Alsaadi, H.; Rangel-Buitrago, N.; Sadooni, F.N. Long-term trends in heavy metal contamination of marine sediments in the Arabian Gulf: A meta-analysis. *Environ. Monit. Assess.* **2025**, *197*, 873. https://doi.org/10.1007/s10661-025-14348-0.
11. Clarizia, L.; Amodeo, L.; Bonsignore, M.; Del Core, M.; Muscetta, M.; Prestigiacomo, C.; Proietto, F.; Manta, D.S.; Traina, A.; D'Agostino, F. Marine sediment remediation under complex contamination: State-of-the-art and perspectives on PAHs, PCBs, and heavy metals. *J. Water Process Eng.* **2026**, *86*, 109761. https://doi.org/10.1016/j.jwpe.2026.109761.
12. Falciglia, P.P.; Malarbì, D.; Vagliasindi, F.G.A. Removal of mercury from marine sediments by the combined application of a biodegradable non-ionic surfactant and complexing agent in enhanced-electrokinetic treatment. *Electrochim. Acta* **2016**, *222*, 1569–1577. https://doi.org/10.1016/j.electacta.2016.11.142.
13. Italian Ministry of the Environment and Protection of Land and Sea. Decree No. 173 of 15 July 2016—Regulation Establishing Procedures and Technical Criteria for the Authorization of the Disposal at Sea of Dredged Materials from Marine Seabeds. Official Gazette of the Italian Republic, General Series No. 208, Supplemento Ordinario No. 40/L, 6 September 2016. Available online: https://www.gazzettaufficiale.it/eli/id/2016/09/06/16G00184/sg (accessed on 7 July 2026).
14. Italian Ministry of the Environment and Protection of Land and Sea. Decree No. 172 of 15 July 2016—Regulation Governing the Procedures and Technical Standards for Dredging Operations at Sites of National Interest, Pursuant to Article 5-Bis, Paragraph 6, of Law No. 84 of 28 January 1994. Official Gazette of the Italian Republic, General Series No. 208, 6 September 2016. Available online: https://www.gazzettaufficiale.it/eli/id/2016/09/06/16G00183/sg (accessed on 7 July 2026).
15. Legislative Decree No. 152 of 3 April 2006—Environmental Regulations (Norme in Materia Ambientale). Official Gazette of the Italian Republic, General Series No. 88, Ordinary Supplement No. 96, 14 April 2006. Available online: https://www.gazzettaufficiale.it/dettaglio/codici/materiaAmbientale (accessed on 14 April 2026).
16. European Commission. The European Green Deal (COM(2019) 640 Final). 2019. Available online: https://eur-lex.europa.eu/legal-content/EN/TXT/?uri=celex:52019DC0640 (accessed on 10 July 2026).
17. Falciglia, P.P.; Malarbì, D.; Roccaro, P.; Vagliasindi, F.G.A. Innovative thermal and physico-chemical treatments for the clean-up of marine sediments dredged from the Augusta Bay (Southern Italy). *Reg. Stud. Mar. Sci.* **2020**, *39*, 101426. https://doi.org/10.1016/j.rsma.2020.101426.
18. Afolayan, A.; Černý, R.; Fořt, J. Review of Treatment Techniques for Dredged Sediments in the Context of Valorization as Secondary Raw Materials. *Buildings* **2025**, *15*, 1639. https://doi.org/10.3390/buildings15101639.
19. Mulligan, C.N.; Yong, R.N.; Gibbs, B.F. An evaluation of technologies for the heavy metal remediation of dredged sediments. *J. Hazard. Mater.* **2001**, *85*, 145–163. https://doi.org/10.1016/S0304-3894(01)00226-6.
20. Deng, T.; Zhang, B.; Li, F.; Jin, L. Sediment washing by EDTA and its reclamation by sodium polyamidoamine-multi dithiocarbamate. *Chemosphere* **2017**, *168*, 450–456. https://doi.org/10.1016/j.chemosphere.2016.09.152.
21. Iannelli, R.; Masi, M.; Ceccarini, A.; Ostuni, M.B.; Lageman, R.; Muntoni, A.; Spiga, D.; Polettini, A.; Marini, A.; Pomi, R. Electrokinetic remediation of metal-polluted marine sediments: Experimental investigation for plant design. *Electrochim. Acta* **2015**, *181*, 146–159. https://doi.org/10.1016/j.electacta.2015.04.093.
22. De Gisi, S.; Todaro, F.; Mesto, E.; Schingaro, E.; Notarnicola, M. Recycling contaminated marine sediments as filling materials by pilot scale stabilization/solidification with lime, organoclay and activated carbon. *J. Clean. Prod.* **2020**, *269*, 122416. https://doi.org/10.1016/j.jclepro.2020.122416.
23. Falciglia, P.P.; Malarbì, D.; Maddalena, R.; Greco, V.; Vagliasindi, F.G.A. Remediation of Hg-contaminated marine sediments by simultaneous application of enhancing agents and microwave heating (MWH). *Chem. Eng. J.* **2017**, *321*, 1–10. https://doi.org/10.1016/j.cej.2017.03.097.
24. Bonomo, L.; Careghini, A.; Dastoli, S.; De Propris, L.; Ferrari, G.; Gabellini, M.; Saponaro, S. Feasibility studies for the treatment and reuse of contaminated marine sediments. *Environ. Technol.* **2009**, *30*, 817–823. https://doi.org/10.1080/09593330902990105.
25. Akcil, A.; Erust, C.; Ozdemiroglu, S.; Fonti, V.; Beolchini, F. A review of approaches and techniques used in aquatic contaminated sediments: Metal removal and stabilization by chemical and biotechnological processes. *J. Clean. Prod.* **2015**, *86*, 24–36. https://doi.org/10.1016/j.jclepro.2014.08.009.
26. Vanthuyne, M.; Maes, A.; Cauwenberg, P. The use of flotation techniques in the remediation of heavy metal contaminated sediments and soils: An overview of controlling factors. *Miner. Eng.* **2003**, *16*, 1131–1141. https://doi.org/10.1016/j.mineng.2003.06.012.
27. Sierra, C.; Menéndez-Aguado, J.M.; Afif, E.; Carrero, M.; Gallego, J.R. Feasibility study on the use of soil washing to remediate the As–Hg contamination at an ancient mining and metallurgy area. *J. Hazard. Mater.* **2011**, *196*, 93–100. https://doi.org/10.1016/j.jhazmat.2011.08.080.

28. Cauwenberg, P.; Verdonckt, F.; Maes, A. Flotation as a remediation technique for heavily polluted dredged material. 1. A feasibility study. *Sci. Total Environ.* **1998**, *209*, 113–119. https://doi.org/10.1016/S0048-9697(98)80102-2.
29. Fečko, P.; Janakova, I.; Raclavská, H.; Tora, B. Application of flotation in the decontamination of sediments from the Cerny prikop stream. *Pol. J. Chem. Technol.* **2009**, *11*, 8–11. https://doi.org/10.2478/v10026-009-0003-4.
30. Bulatovic, S.M. Chemistry, theory and practice: Flotation of Sulphide Ores. In *Handbook of Flotation Reagents*, 1st ed.; Elsevier: Amsterdam, The Netherlands, 2007.
31. Fuerstenau, M.C.; Jameson, G.J.; Yoon, R.H. *Froth Flotation: A Century of Innovation*; Society for Mining, Metallurgy, and Exploration: Littleton, CO, USA, 2007.
32. Wills, B.A.; Finch, J.A. *Wills' Mineral Processing Technology. An Introduction to the Pratical Aspects of Ore Treatment and Mineral Recovery*, 8th ed.; Elsevier: Amsterdam, The Netherlands, 2016.
33. Manca, P.P.; Massacci, G.; Pintus, D.; Sogos, G. The flotation of sphalerite mine tailings as a remediation method. *Miner. Eng*. **2021**, *165*, 106862. https://doi.org/10.1016/j.mineng.2021.106862.
34. Cauwenberg, P.; Verdonckt, F.; Maes, A. Flotation as a remediation technique for heavily polluted dredged material. 2. Characterisation of flotated fractions 11. *Sci. Total Environ.* **1998**, *209*, 121–131. https://doi.org/10.1016/S0048-9697(98)80103-4.
35. Chipfunhu, D.; Bournival, G.; Dickie, S.; Ata, S. Performance characterisation of new frothers for sulphide mineral flotation. *Miner. Eng*. **2019**, *131*, 272–279. https://doi.org/10.1016/j.mineng.2018.11.014.
36. Veetil, D.P.; Mercier, G.; Blais, J.-F.; Chartier, M. Optimization of Operating Parameters for the Selective Flotation of Heavy Metals from Contaminated Fine Sediment Using Response Surface Model. *Soil Sediment Contam.* **2014**, *23*, 107–125. https://doi.org/10.1080/15320383.2013.783556.
37. Mankosa, M.J.; Kohmuench, J.N.; Christodoulou, L.; Luttrell, G.H. Recovery of values from a porphory copper tailings stream. In Proceedings of the 28th International Mineral Processing Congress (IMPC), Quebec City Convention Center, Quebec, QC, Canada, 11–15 September 2016; paper 457, 10p.
38. Lee, J.Y.; Kim, G.Y.; Kang, N.K.; Yi, B.Y.; Jung, J.W.; Im, J.H.; Son, B.K.; Bahk, J.J.; Chun, J.H.; Ryu, B.J.; et al. Physical properties of sediments from the Ulleung Basin, East Sea: Results from Second Ulleung Basin Gas Hydrate Drilling Expedition, East Sea (Korea). *Mar. Pet. Geol.* **2013**, *47*, 43–55. https://doi.org/10.1016/j.marpetgeo.2013.05.017.
39. Chu, S.H.; Yao, J.J. A strength model for concrete made with marine dredged sediment. *J. Clean. Prod.* **2020**, *274*, 122673. https://doi.org/10.1016/j.jclepro.2020.122673.
40. Wang, H.; Wang, Z.; Yang, W.; Jia, H.; You, Z. Characterization, pollution, and beneficial utilization assessment of dredged sediments from coastal ports in China. *Mar. Pollut. Bull.* **2025**, *211*, 117389. https://doi.org/10.1016/j.marpolbul.2024.117389.
41. Trahar, W.J. A rational interpretation of the role of particle-size in flotation. *Int. J. Miner. Process.* **1981**, *8*, 289–327. https://doi.org/10.1016/0301-7516(81)90019-3.
42. Miettinen, T.; Ralston, J.; Fornasiero, D. The limits of fine particle flotation. *Miner. Eng.* **2010**, *23*, 420–437. https://doi.org/10.1016/j.mineng.2009.12.006.
43. Chipfunhu, D.; Zanin, M.; Grano, S. The dependency of the critical contact angle for flotation on particle-size—Modelling the limits of fine particle flotation. *Miner. Eng.* **2011**, *24*, 50–57. https://doi.org/10.1016/j.mineng.2010.09.020.
44. Farrokhpay, S.; Filippov, L.; Fornasiero, D. Flotation of Fine Particles: A Review. *Miner. Process. Extr. Metall. Rev.* **2021**, *42*, 473–483. https://doi.org/10.1080/08827508.2020.1793140.
45. Ghasemi Flavarjani, M.H.; Sobouti, A.; Rezai, B.; Ahmadi, A. A review of fine particle flotation: Mechanistic insights and advances. *Miner. Eng.* **2025**, *234*, 109685. https://doi.org/10.1016/j.mineng.2025.109685.
46. Dermont, G.; Bergeron, M.; Mercier, G.; Richer-Laflèche, M. Soil washing for metal removal: A review of physical/chemical technologies and field applications. *J. Hazard. Mater*. **2008**, *152*, 1–31. https://doi.org/10.1016/j.jhazmat.2007.10.043.
47. Moimane, T.; Peng, Y. Sulphidisation of oxides and oxidised sulphides and adsorption of thiol collectors on the sulphidised products-a critical review. *Adv. Colloid. Interface Sci.* **2022**, *305*, 102697. https://doi.org/10.1016/j.cis.2022.102697.
48. Chen, Y.; Sun, Y.; Han, Y. Efficient flotation separation of lead–zinc oxide ores using mineral sulfidation reconstruction technology: A review. *Green Smart Min. Eng.* **2024**, *1*, 175–189. https://doi.org/10.1016/j.gsme.2024.05.004.
49. Veetil, D.P.; Mercier, G.; Blais, J.F.; Chartier, M.; Tran, L.H.; Taillard, V. Remediation of Contaminated Dredged Sediments Using Physical Separation Techniques. *Soil Sediment Contam.* **2014**, *23*, 932–953. https://doi.org/10.1080/15320383.2014.896860.
50. Rahman, M.K.A.E.; Maes, A.; Cauwenberg, P. Removal of Heavy Metal Impurities from Dredged River Sediment. *Chem. Eng. Technol.* **1999**, *22*, 707–712. https://doi.org/10.1002/(SICI)1521-4125(199908)22:8<707::AID-CEAT707>3.0.CO;2-Y.
51. Burton, E.D.; Phillips, I.R.; Hawker, D.W. Factors Controlling the Geochemical Partitioning of Trace Metals in Estuarine Sediments. *Soil Sediment Contam.* **2006**, *15*, 253–276. https://doi.org/10.1080/15320380600646290.

52. Wei, Q.; Dong, L.; Qin, W.; Jiao, F.; Qi, Z.; Feng, C.; Sun, D.; Wang, L.; Xiao, S. Efficient Flotation Recovery of Lead and Zinc from Refractory Lead-Zinc Ores under Low Alkaline Conditions. *Geochemistry* **2021**, *81*, 125769. https://doi.org/10.1016/j.chemer.2021.125769.
53. Boar, P.L.; Ingram, L.K. The comprehensive analysis of coal ash and silicate rocks by atomic-absorption spectrophotometry by a fusion technique. *Analyst* **1970**, *95*, 124–130. https://doi.org/10.1039/an9709500124.
54. *EN 15935:2021*; Soil, Waste, Treated Biowaste and Sludge—Determination of Loss on Ignition. European Committee for Standardization (CEN): Brussels, Belgium, 2021.
55. USEPA (United States Environmental Protection Agency). SW-846 Test Method 3052: Microwave Assisted Acid Digestion of Silceous and Organically Based Matrices. 1996. 20p. Available online: https://www.epa.gov/sites/default/files/2015-12/documents/3052.pdf (accessed on 4 November 2025).
56. Mossop, K.F.; Davidson, C.M. Comparison of original and modified BCR sequential extraction procedures for the fractionation of copper, iron, lead, manganese and zinc in soils and sediments. *Anal. Chim. Acta* **2003**, *478*, 111–118. https://doi.org/10.1016/S0003-2670(02)01485-X.
57. Mifsud, J.; Spiridonov, P.; Statsenko, L.; Abaka-Wood, G.; Styan, C.; Asamoah, R. Sediment Remediation in Port Pirie River: Process Development and Cost Reduction. In *Proceedings of the Australasian Coasts & Ports 2025 Conference*; Engineers Australia: Adelaide, Australia, 2025; pp. 440–449.
58. Babel, B.; Penz, M.; Schach, E.; Boehme, S.; Rudolph, M. Reprocessing of a Southern Chilean Zn Tailing by Flotation—A Case Study. *Minerals* **2018**, *8*, 295. https://doi.org/10.3390/min8070295.
59. Drif, B.; Taha, Y.; Hakkou, R.; Benzaazoua, M. Recovery of Residual Silver-Bearing Minerals from Low-Grade Tailings by Froth Flotation: The Case of Zgounder Mine, Morocco. *Minerals* **2018**, *8*, 273. https://doi.org/10.3390/min8070273.
60. Liao, Z.; Jia, W.; Luo, J.; Wang, X.; Chen, W. Study on Occurrence States of Low-Grade Cu-Zn in Iron Tailings and Changes in Production Flowsheet. *Minerals* **2026**, *16*, 131. https://doi.org/10.3390/min16020131.
61. Cherchi, A.; Da Pelo, S.; Ibba, A.; Mana, D.; Buosi, C.; Floris, N. Benthic foraminifera response and geochemical characterization of the coastal environment surrounding the polluted industrial area of Portovesme (South-Western Sardinia, Italy). *Mar. Pollut. Bull.* **2009**, *59*, 281–296. https://doi.org/10.1016/j.marpolbul.2009.09.016.
62. Schintu, M.; Degetto, S. Sedimentary records of heavy metals in the industrial harbour of Portovesme, Sardinia (Italy). *Sci. Total Environ*. **1999**, *241*, 129–141. https://doi.org/10.1016/S0048-9697(99)00336-8.
63. Peres, A.E.C.; Borges, A.A.M.; Galery, R. The effect of the dispersion degree of the floatability of an oxidised zinc ore. *Miner. Eng*. **1994**, *7*, 1435–1439. https://doi.org/10.1016/0892-6875(94)00081-6.
64. Ejtemaei, M.; Gharabaghi, M.; Irannajad, M. A review of zinc oxide mineral beneficiation using flotation method. *Adv. Colloid Interface Sci*. **2014**, *206*, 68–78. https://doi.org/10.1016/j.cis.2013.02.003.
65. Rahman, R.M.; Ata, S.; Jameson, G.J. The effect of flotation variables on the recovery of different particle size fractions in the froth and the pulp. *Int. J. Miner. Process.* **2012**, *106–109*, 70–77. https://doi.org/10.1016/j.minpro.2012.03.001.
66. Norori-McCormac, A.; Brito-Parada, P.R.; Hadler, K.; Cole, K.; Cilliers, J.J. The effect of particle size distribution on froth stability in flotation. *Sep. Purif. Technol.* **2017**, *184*, 240–247. https://doi.org/10.1016/j.seppur.2017.04.022.
67. Mackay, I.; Mendez, E.; Molina, I.; Videla, A.R.; Cilliers, J.J.; Brito-Parada, P.R. Dynamic froth stability of copper flotation tailings. *Miner. Eng.* **2018**, *124*, 103–107. https://doi.org/10.1016/j.mineng.2018.05.005.
68. Mackay, I.; Videla, A.R.; Brito-Parada, P.R. The link between particle size and froth stability—Implications for reprocessing of flotation tailings. *J. Clean. Prod.* **2020**, *242*, 118436. https://doi.org/10.1016/j.jclepro.2019.118436.
69. Huang, X.; Wang, Z.; Deng, B.; Chen, R.; Zhou, M.; He, X.; Mi, S.; Lan, C.; Wang, J. Understanding the influence of fine particles on froth stability in smithsonite flotation (systems). *Miner. Eng.* **2026**, *244*, 110291. https://doi.org/10.1016/j.mineng.2026.110291.
70. Awatey, B.; Thanasekaran, H.; Kohmuench, J.N.; Skinner, W.; Zanin, M. Optimization of operating parameters for coarse sphalerite flotation in the HydroFloat fluidised-bed separator. *Miner. Eng.* **2013**, *50–51*, 99–105. https://doi.org/10.1016/j.mineng.2013.06.015.
71. Janishar Anzoom, S.; Bournival, G.; Ata, S. Coarse particle flotation: A review. *Miner. Eng.* **2024**, *206*, 108499. https://doi.org/10.1016/j.mineng.2023.108499.
72. Mehdilo, A.; Irannajad, M.; Zarei, H. Flotation of zinc oxide ore using cationic and cationic-anionic mixed collectors. *Physicochem. Probl. Miner. Process.* **2013**, *49*, 145–156. https://doi.org/10.5277/PPMP130114.
73. Ralston, J.; Hayes, R.A.; Fornasiero, D. Bubble–particle attachment and detachment in flotation. *Int. J. Miner. Process.* **1999**, *56*, 133–164. https://doi.org/10.1016/S0301-7516(98)00046-5.

74. Zheng, G.; Nguyen, A.V.; Nguyen, T.A.H.; Nguyen, N.N.; Ma, L. Advancing models of bubble-particle contact times: A comprehensive review of flotation attachment efficiency prediction. *Adv. Colloid Interface Sci.* **2025**, *345*, 103609. https://doi.org/10.1016/j.cis.2025.103609.
75. Pawliszak, P.; Bradshaw-Hajek, B.H.; Skinner, W.; Beattie, D.A.; Krasowska, M. Frothers in flotation: A review of performance and function in the context of chemical classification. *Miner. Eng.* **2024**, *207*, 108567. https://doi.org/10.1016/j.mineng.2023.108567.
76. Chandra, A.P.; Gerson, A.R. A review of the fundamental studies of the copper activation mechanisms for selective flotation of the sulfide minerals, sphalerite and pyrite. *Adv. Colloid Interface Sci.* **2009**, *145*, 97–110. https://doi.org/10.1016/j.cis.2008.09.001.
77. Liu, R.; Pei, B.; Liu, Z.; Wang, Y.; Li, J.; Liu, D. Improved Understanding of the Sulfidization Mechanism in Amine Flotation of Smithsonite: An XPS, AFM and UV–Vis DRS Study. *Minerals* **2020**, *10*, 370. https://doi.org/10.3390/min10040370.
78. Wang, M.; Wei, H.; Jin, S.; Zhang, G. Effect of Pre-Sulfidization on the Octadecyl Amine Adsorption on the Smithsonite Surface and Its Flotation. *Molecules* **2024**, *29*, 3921. https://doi.org/10.3390/molecules29163921.
79. Ri, K.; Ri, J.; Kim, K.; Ri, H.; Song, R.; Kim, C. Application of flotation on the recovery/removal of heavy metals in secondary resources: A comprehensive review. *Miner. Eng.* **2024**, *218*, 108999. https://doi.org/10.1016/j.mineng.2024.108999.

Disclaimer/Publisher's Note: The statements, opinions and data contained in all publications are solely those of the individual author(s) and contributor(s) and not of MDPI and/or the editor(s). MDPI and/or the editor(s) disclaim responsibility for any injury to people or property resulting from any ideas, methods, instructions or products referred to in the content.